Electron T 1 measurements in short-lived free radicals by dynamic polarization recovery

D. M. Bartels, R. G. Lawler, and A. D. Trifunac

Citation: The Journal of Chemical Physics **83**, 2686 (1985); doi: 10.1063/1.449271
View online: http://dx.doi.org/10.1063/1.449271
View Table of Contents: http://scitation.aip.org/content/aip/journal/jcp/83/6?ver=pdfcov
Published by the AIP Publishing

Electron T_1 measurements in short-lived free radicals by dynamic polarization recovery[a)]

D. M. Bartels and R. G. Lawler
Chemistry Department, Brown University, Providence, Rhode Island 02912

A. D. Trifunac
Chemistry Division, Argonne National Laboratory, Argonne, Illinois 60439

(Received 25 April 1985; accepted 5 June 1985)

A dynamic polarization recovery method for measurement of electron spin T_1 relaxation times in free radicals in liquids is described, which is valid even in the presence of chemically induced dynamic electron polarization (CIDEP) and fast chemical decay of the radicals. The method is based on pulsed microwave perturbation and detection of transient magnetization following radical creation in a short pulse. Analysis of the experimental approach and a theoretical description of the method is presented together with a detailed discussion of the advantages and the limitations of the technique. Electron T_1 measurements are presented for 14 short-lived free radicals generated in aqueous solution. The magnitudes of the observed relaxation times, which range from 0.1 to 4 μs, are discussed within the framework of current theories of relaxation for small radicals in liquids. It is tentatively concluded that the spin rotation mechanism is responsible for the very short T_1's in this series of radicals.

I. INTRODUCTION

It has long been recognized that the study of electron spin relaxation of free radicals in solution can yield information about the dynamics of molecular tumbling, solvent–radical interactions, ion pairing, and radical–radical collisions.[1] Spin-label relaxation measurements have recently proven particularly useful in systems of biological interest.[2] The methodology for these measurements is now well established and experiments on long-lived free radicals are fairly routine.[3,4]

Accurate knowledge of relaxation times for short-lived free radical intermediates is also very desirable, both as a probe of structure and because relaxation plays an important role in determining the dynamic behavior of signals observed in time-resolved EPR experiments.[5–9] Time-resolved EPR in turn may reveal a great deal about reaction mechanisms and diffusion-controlled processes in liquids.[9,10]

In extensions of recent studies of Heisenberg exchange and electron spin polarization (CIDEP) in free radicals created by *in situ* pulse radiolysis of aqueous solutions,[11,12] we have found it essential to obtain independent estimates of the longitudinal electron spin relaxation time T_1 in order to interpret the observed CIDEP enhancements. Consequently, we have developed a dynamic polarization recovery technique to directly measure T_1 in rapidly decaying radical samples which also exhibit CIDEP effects. It is the purpose of this paper to describe this method, which should be generally applicable to reactive free radicals produced in short pulses.

To date, few relaxation studies of highly reactive and therefore short-lived radicals have been published, due in large part to the difficulty of generating sufficiently high concentrations of such species. The first accurate estimates of T_1 for transient radicals made use of traditional cw progressive saturation methods,[13] which may be employed even with very small steady-state concentrations of unpaired electron spins.[14] However, saturation recovery experiments[3,4] have called into question the validity of progressive saturation results in some stable radical systems, and the interpretation of cw experiments in the presence of fast chemical decay processes may be even more uncertain.

Fast response EPR spectrometers interfaced with pulsed radical sources have become available in recent years,[7,13,15,16] allowing the magnetization of transient radicals to be followed directly in the time domain as the radicals are formed and disappear in chemical reactions. Analysis of time-resolved EPR signals obtained using high frequency field modulation or direct detection of radicals produced by pulse radiolysis or flash photolysis have yielded T_1 estimates in a few cases.[6,17,18] In these experiments, however, the samples usually exhibit CIDEP effects and transient nutations which must be accounted for by fitting several parameters (notably the microwave power level and inhomogeneous contributions to the linewidth) in addition to the desired T_1. Fessenden *et al.*[19] recently extended saturation recovery methodology to transient radicals produced by continuous *in situ* electron beam irradiation. Their technique shows some promise of general utility, but suffers both from sensitivity problems associated with the continuous irradiation method and from the appearance of transient nutations at the microwave power levels necessary for the experiment. With the exception of atomic hydrogen, only relatively long-lived free radicals have so far been studied by this technique. The laser flash photolysis method developed by McLauchlan and co-workers[20–27] has provided the largest number of

[a)] Work at Argonne and Brown University performed under the auspices of the Office of Basic Energy Sciences, Division of Chemical Science, US-DOE under Contract Nos. W-31-109-ENG-38 and DE-AC02-82ER12042, respectively.

 0021-9606/85/182686-22$02.10

direct T_1 measurements to date. This technique exploits the large uniform polarization of EPR lines generated via the triplet mechanism of CIDEP. Initial experiments employed 2 MHz field modulation and required that $T_1 \gg T_2$ in order to obtain a simple relationship between the signal intensity and T_1.[20–23] Direct detection methods have since removed this restriction,[24–26] and very recently it was shown that further simplification could be obtained by gating of the microwaves after the laser flash.[27] The technique is limited, of course, to free radicals which can be created photochemically with large initial polarizations. The recent use of rapidly modulated light sources coupled with phase sensitive EPR detection also shows some promise for yielding accurate T_1 values, but requires multiple parameter fitting as with the other methods mentioned above.[28]

The approach to T_1 measurement in transient species to be described here takes advantage of the large radical populations which can be generated by pulse radiolysis (or laser photolysis) and the fast time response afforded by pulsed EPR detection methods. The basic idea is to create a large population of free radicals with a pulse of electrons (or photons), perturb the polarization of a resonant EPR transition with a high power microwave pulse, and observe the magnetization as it recovers to the "unperturbed" (but not necessarily equilibrium) magnetization which is characteristic of the chemistry in the system. Fast time response and good sensitivity are conveniently obtained by probing the magnetization with short microwave pulses by the technique of free induction decay (FID) integration.[8] T_1 information can be recovered using only a two-parameter least-squares fit by comparing the "perturbed" magnetization with the signal present in the absence of the perturbation pulse. We call this method "dynamic polarization recovery" to indicate that the signal does not reach a steady-state value as in traditional saturation or inversion-recovery experiments, but recovers to a dynamic polarization which depends on when the perturbing microwave pulse is applied after the radical creation event.

The principal advantage of the FID-detected polarization recovery method lies in its insensitivity to precise knowledge or control of microwave field (H_1) amplitudes or magnetic field homogeneity. It is only required that the amplitudes of the perturbation and probe pulses be reproducible at a given position in the sample. This avoids the need to employ the effective microwave field at the sample as a fitting parameter. In addition, the excitation and detection phases of the experiment are well separated in time, which simplifies the way in which corrections for reaction and CIDEP are incorporated into the analysis of recovery curves. The need for only a two-parameter least-squares fit is a significant advance over the multiple-parameter fits needed with other approaches.[6,24,27]

The pulsed EPR detection techniques (FID or spin echo) are well suited to the study of small reactive free radicals, which generally exhibit simple EPR spectra consisting of a few well-resolved hyperfine lines. Radicals or chemical systems with closely spaced, nondegenerate lines are difficult to investigate more than qualitatively by this method, however, because of interference of the FID signals from on-resonance and slightly off-resonance portions of the spectrum. For simple spectra, it is presently possible to measure recovery times as short as 200 ns in the presence of chemical half-lives on the order of 1 μs, or T_1, whichever is longer. More qualitative measurements can be made when T_1 and T_2 are as short as 100 ns.

Section II presents a theoretical description of the dynamic polarization recovery method, based on the modified Bloch equations commonly used in time-resolved EPR studies. The basic experiment is justified first, using a number of simplifying assumptions. The remainder of Sec. II examines in more detail the conditions for validity of the method. Section III describes the apparatus and outlines the radiation chemistry used for generation of free radicals in aqueous solution. In Sec. IV, results are tabulated for a series of radicals created in aqueous solution from simple inorganic reagents, organic acids, and alcohols, with T_1's in the range of 0.1–3.5 μs. A general discussion of the results in terms of the relevant theoretical concepts of electron spin relaxation is presented in Sec. V.

II. THEORY

A. Magnetization in a reacting system

EPR detection of highly reactive free radicals in solution generally requires that the radicals be created *in situ* in an EPR spectrometer by photolysis or radiolysis. The magnetization $\mathbf{M}$ detected in such an experiment may deviate substantially from equilibrium and is always strongly coupled to the chemical kinetics of the reacting system. At the magnetic fields used in X-band EPR spectroscopy, the majority of organic and some inorganic free radicals exhibit hyperfine structure, each component of which, $\mathbf{M}_\lambda$, may be described approximately by a modified Bloch equation of the form[5–9]

$$\dot{\mathbf{M}}_\lambda = (\dot{\mathbf{M}}_\lambda^0) + (\dot{\mathbf{M}})_\lambda^{\mathrm{GEN}} + (\dot{\mathbf{M}})_\lambda^{\mathrm{RXN}} + (\dot{\mathbf{M}})_\lambda^{\mathrm{RPM}} + (\dot{\mathbf{M}})_\lambda^{\mathrm{HE}}. \tag{1}$$

In this equation, $(\dot{\mathbf{M}})_\lambda^0$ represents the terms of the unmodified Bloch equations, including intramolecular relaxation and interactions with magnetic fields, $(\dot{\mathbf{M}})_\lambda^{\mathrm{GEN}}$ describes the generation of initial magnetization coincident with free radical creation, and $(\dot{\mathbf{M}})_\lambda^{\mathrm{RXN}}$ corresponds to loss of magnetization as the free radicals react. The second and third terms are expected to be virtually the same for all hyperfine components,[10] and the first term dependent on λ only through coupled electron–nuclear relaxation. On the other hand, the terms $(\dot{\mathbf{M}})_\lambda^{\mathrm{RPM}}$ and $(\dot{\mathbf{M}})_\lambda^{\mathrm{HE}}$ describe the polarizing effects of radical pair mechanism CIDEP and the relaxation effects of Heisenberg exchange, respectively, and often vary markedly from one hyperfine component to another. In addition, the exchange term has the effect of coupling the equations for different λ, so that a complete description of the entire free radical ensemble requires solution of $3N$ coupled equations, where N is the total number of nuclear spin states.[10,12]

Since we will be primarily interested in the deviation of the spin system from thermal equilibrium, it is convenient to write the magnetization in terms of a unitless vector $\mathbf{P}_\lambda(t)$ and the hypothetical equilibrium magnetization $M_z^0(t)$

which is proportional to the chemical concentration[7] $[M_z^0(t) \propto R(t)]$:

$$(\dot{\mathbf{M}})_\lambda(t) = M_z^0(t)\mathbf{P}_\lambda(t). \tag{2}$$

It follows from this definition that

$$(\dot{\mathbf{M}})_\lambda = (\dot{M})_z^0(t)\mathbf{P}_\lambda(t) + M_z^0(t)\dot{\mathbf{P}}_\lambda(t). \tag{3}$$

If it is assumed[29] that the chemical decay of $\mathbf{M}_\lambda$ is proportional to the decrease in free radical concentration, we have

$$(\dot{\mathbf{M}})_\lambda^{\mathrm{RXN}} = \frac{\dot{R}(t)}{R(t)}\mathbf{M}_\lambda = \frac{\dot{M}_z^0}{M_z^0}\mathbf{M}_\lambda = \dot{M}_z^0\,\mathbf{P}_\lambda, \tag{4}$$

and substitution of Eqs. (2)–(4) into Eq. (1) leads to the following equation for $\dot{\mathbf{P}}_\lambda$:

$$\dot{\mathbf{P}}_\lambda = (\dot{\mathbf{P}})_\lambda^0 + (\dot{\mathbf{P}})_\lambda^{\mathrm{GEN}} + (\dot{\mathbf{P}})_\lambda^{\mathrm{RPM}} + (\dot{\mathbf{P}})_\lambda^{\mathrm{HE}}. \tag{5}$$

The effect of this substitution is to normalize the magnetization for the instantaneous free radical concentration so that the resulting equations for $\dot{\mathbf{P}}_\lambda$ more nearly correspond to the Bloch equations in the absence of chemical reactions. Note that by the definition of $\mathbf{P}_\lambda$, the equilibrium condition in the absence of a resonant microwave field is $P_{x\lambda} = P_{y\lambda} = 0$ and $P_{z\lambda} = 1$. The z component of $\mathbf{P}_\lambda$ can therefore be thought of as a relative polarization $P_{z\lambda} = p_\lambda/p_\lambda^0$ for the hyperfine component λ, where the absolute polarization p_λ is commonly expressed in terms of sums and differences of the number of spins in the two electron spin states[30]: $p = (n\downarrow - n\uparrow)/(n\downarrow + n\uparrow)$. The equilibrium polarization p_λ^0 is about 10^{-3} at room temperature in the field of an X-band EPR spectrometer. Because of the close connection between $\mathbf{P}_\lambda$ and the polarization p_λ, we will refer to $\mathbf{P}_\lambda$ as the "polarization vector" in the discussion that follows.

The dynamic polarization recovery experiment to be described in the following sections assumes that free radicals are created in a pulse on a time scale which is short compared to their subsequent chemical decay. Consequently, it is appropriate for this discussion to drop the generation term $(\dot{\mathbf{P}})_\lambda^{\mathrm{GEN}}$ and include its contribution later as an initial condition. A further simplification results from the use of a pulsed microwave detection scheme,[7,8] since the longitudinal and transverse magnetization are uncoupled except during the microwave pulses. The y magnetization is detected at time $t+\tau$ after the end of a pulse sequence initiated at time t. The signal may often be interpreted in terms of the product

$$S(t,\tau) = M_z(t)\cdot C(t,\tau), \tag{6}$$

where $M_z(t)$ is the longitudinal magnetization at the time of a short probe pulse and $C(t,\tau)$ reflects changes in the resulting transverse magnetization occurring between t and $t+\tau$.[11,12] $C(t,\tau)$ may represent either a free induction decay (FID) signal or the amplitude of a spin echo generated with a second microwave pulse. If both the length of the probe pulse and the delay time τ are sufficiently short, $C(t,\tau)$ becomes independent of t $[C(t,\tau) \simeq \text{constant}]$, and the time profile of $S(t,\tau)$ is a true representation of $M_z(t)$. [The form of the function $C(t,\tau)$ at high free radical concentrations actually provides a sensitive probe of the Heisenberg exchange term of Eq. (1), and will be the subject of a future paper.[31]]

In the limit that Eq. (6) is valid and $C(t,\tau)$ is constant, we need only consider the development of $M_z(t)$ in the periods between microwave pulses. In Sec. II B, therefore, we find a general solution of Eq. (5) which is valid in the absence of a microwave field. In Sec. II C we will use this result to show how T_1 information may easily be obtained in a pulsed experiment even in the presence of CIDEP and fast chemical decay of the sample. The subsequent sections treat the assumptions in more detail. Section II D examines the behavior of the polarization vector $\mathbf{P}_\lambda(t)$ upon application of a microwave pulse in order to determine the conditions for validity of Eq. (6). Finally, in Sec. II E, we consider the effects of nonideal microwave pulses, inhomogeneous samples, and multiple-radical systems on the dynamic polarization recovery experiment.

B. Magnetization in the absence of a microwave field

In the periods between microwave pulses the polarization of an ensemble containing only one free radical species will be governed by the z component of Eq. (5), which can be written explicitly in the form[32]

$$\dot{\mathbf{P}}_{z\lambda} = \frac{-1}{T_1}(P_{z\lambda} - 1) + E_\lambda k_r R(t) - \frac{k_{ex}R(t)}{N}\sum_{\mu=1}^{N}(P_{z\lambda} - P_{z\mu}). \tag{7}$$

In this equation, k_r is the second-order reaction rate constant and k_{ex} is the second-order rate constant for Heisenberg exchange, both of which are assumed to be independent of λ. E_λ is the intrinsic CIDEP enhancement factor for the EPR line in question. The last term of Eq. (7) describes the Heisenberg exchange contribution, which couples all of the N hyperfine components together.

Given the assumption that T_1 is independent of λ,[33] one can sum over all of the N separate hyperfine components and make use of the well-known RPM identity[5] $\Sigma_{\lambda=1}^{N} E_\lambda = 0$ to arrive at an equation for the average polarization of the ensemble:

$$\frac{1}{N}\sum_{\lambda=1}^{N}\dot{\mathbf{P}}_{z\lambda} = \dot{\overline{P}} = -\frac{1}{T_1}(\overline{P} - 1). \tag{8}$$

This equation is easily solved and one obtains

$$\frac{1}{N}\sum_{\lambda=1}^{N} P_{z\lambda} = \overline{\mathbf{P}} = 1 + [\overline{P}(t_0) - 1] \times \exp\{-(t - t_0)/T_1\}. \tag{9}$$

Equation (9) shows that the average polarization behaves as expected for an ensemble of noninteracting spins, with the initial polarization $\overline{P}(t_0)$ decaying to the equilibrium value with time constant T_1. Moreover, for radicals created with equilibrium polarization, as is expected for radicals formed from hydroxyl,[6] $\overline{P} = 1$ at all times. Substituting this result into Eq. (7) simplifies the Heisenberg exchange term and decouples the system of N equations:

$$\dot{\mathbf{P}}_{z\lambda} = -\frac{1}{T_1} - (P_{z\lambda} - 1) + E_\lambda k_r R(t) - k_{ex}R(t)(P_{z\lambda} - 1). \tag{10}$$

Equation (10) has the formal solution

$$P_{z\lambda}(t) = 1 + [P_{z\lambda}(t_0) - 1] \exp\left[-\int_{t_0}^{t} [T_1^{-1} + k_{ex} R(t')]\, dt' \right] + V_\lambda(t), \quad (11)$$

where

$$V_\lambda(t) = E_\lambda \int_{t_0}^{t} dt'\, k_r R(t') \times \exp\left[-\int_{t'}^{t} dt''\, [T_1^{-1} + k_{ex} R(t'')] \right],$$

and $P_{z\lambda}(t_0)$ is the polarization at some time t_0.

C. Extracting T_1 from pulsed experiments

In principle, Eq. (11) can be used to determine the interesting molecular properties T_1, k_{ex}, and $k_r \cdot E_\lambda$ if $R(t)$ is known by some independent method. In practice, however, this implies the use of four or five fitting parameters which almost never gives a unique fit of experimental data. Consequently, it is necessary to obtain independent measurements of some parameters to use in the more general calculation. The form of Eq. (11) suggests several ways to estimate T_1, especially if the boundary condition $P_{z\lambda}(t_0)$ is known. We will now proceed to define a number of cases and suggest methods for extracting T_1 information from the signal obtained in a pulsed EPR experiment.

1. The special case of low concentration and initial polarization

Inspection of Eq. (11) shows that if $R(t)$ is nearly constant over several T_1 periods following t_0, an initial polarization $P_{z\lambda}(t_0)$ decays exponentially to equilibrium with a rate constant given by $1/T_1 + k_{ex}\mathrm{R(t)}$. If $P_{z\lambda}(t_0)$ is much greater than unity, and if $k_{ex} R(t) \ll T_1^{-1}$, then the signal will closely resemble a simple exponential decay with time constant T_1. This is the essence of the method used extensively by McLauchlan and co-workers[20–27] in systems where a large initial polarization is generated by triplet mechanism CIDEP. Alternatively, if $P_{z\lambda}(t_0) \simeq 0$ and $R(t)$ is nearly constant, the magnetization signal following t_0 will resemble an exponential rise toward equilibrium. [If $R(t)$ decays slowly in a pulsed experiment, the reaction rate $k_r R(t)$ must be small and $V_\lambda(t)$ should be negligible.] This boundary condition was used by Verma and Fessenden[6,17] to estimate T_1 values for several free radicals formed by scavenging (unpolarized) solvated electrons. In either case outlined above, it should be possible to directly fit the data obtained in a pulsed experiment with one or two parameters, since the kinetics are dominated by T_1. Unfortunately, neither boundary condition pertains to our experiments, since radicals are created by reaction with $\cdot$OH (or $\cdot O^-$) which reaches equilibrium in less than 1 ns and transfers equilibrium polarization to the secondary radicals.[6]

2. Saturation recovery of unpolarized lines

While it is not always possible to generate a well-defined nonequilibrium polarization in the radical creation process, it is possible to generate the boundary condition $P_{z\lambda}(t_0) = 0$ with a saturating microwave pulse when t_0 corresponds to the end of the saturation pulse. The recovery of the polarization from saturation is described by Eq. (11) where it is understood that $t \geqslant t_0$. This experiment is illustrated schematically in Fig. 1. By comparing the saturation recovery signal S_{REC} with the signal detected in the absence of a saturating pulse, S_{REF}, it becomes possible to obtain a direct measurement of T_1, *even in the presence of fast chemical decay of the radicals.*

The comparison is particularly straightforward in the case of radicals which possess a central line, for which $V_\lambda(t) = 0$. Combination of Eqs. (6) and (11) then gives for the recovery curve

$$S_{\mathrm{REC}}(t - t_0) = M_z^0 \left(1 - \exp\left\{ -\int_{t_0}^{t} dt' \, [T_1^{-1} + k_{ex} R(t)] \right\}\right) C(t,\tau). \quad (12)$$

A similar equation for the signal in the absence of the saturation pulse is

$$S_{\mathrm{REF}}(t - t_0) = M_z^0(t) C(t,\tau), \quad (13)$$

where we have assumed $P_{z\lambda}(t_0) = 1$, i.e., initial equilibrium polarization for the center line. If $T_1^{-1} \gg k_{ex} R(t_0)$, the ratio of the two curves is given by

$$\frac{S_{\mathrm{REC}}(t - t_0)}{S_{\mathrm{REF}}(t - t_0)} = 1 - \exp\{ -(t - t_0)/T_1 \}. \quad (14)$$

This result applies regardless of the actual form of $R(t)$, which may involve any number of competing chemical reactions. Consequently, T_1 for this radical may be extracted by performing only two time-resolved experiments, taking a point-by-point ratio of the data, and fitting the result to a simple exponential function.

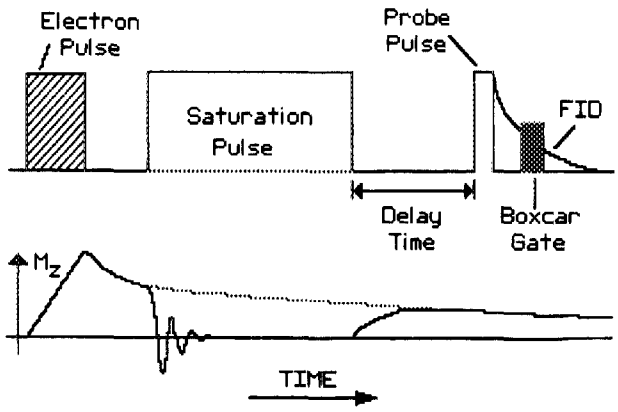

FIG. 1. Schematic outline of a dynamic saturation recovery experiment. The upper half of the figure shows the pulse sequence for free radical creation, saturation of an EPR transition, and detection of magnetization by the FID integration method. In the lower half of the figure the corresponding behavior of M_z is plotted. The dotted curve indicates the magnetization in the absence of a saturation pulse. Following a saturation pulse, M_z recovers over a period of $\sim 5T_1$ toward the time-dependent (often non-Boltzmann) magnetization, which is characteristic of the chemistry of the system.

3. General polarization recovery method

Estimating T_1 for radicals with no unpolarized center line is only slightly more difficult. The ratio S_{REC}/S_{REF} for polarized lines also tends toward unity after several T_1 periods (dynamic polarization recovery), but the apparent time constant of the recovery may differ significantly from T_1 due to the enhancement term $V_\lambda(t)$. It is possible to eliminate the enhancement term by taking the difference of the polarization recovery and reference curves. Assuming $T_1^{-1} \gg k_{ex}R(t_0)$, combination of Eqs. (6) and (11) gives

$$S_{REF}(t-t_0) - S_{REC}(t-t_0) = M_z^0(t)\Delta P_{z\lambda}(t_0)\exp\{-(t-t_0)/T_1\}C(t,\tau), \quad (15)$$

where

$$\Delta P_{z\lambda}(t_0) = [P_{z\lambda}(t_0)]_{REF} - [P_{z\lambda}(t_0)]_{REC}.$$

For ideal saturation recovery experiments, $[P_{z\lambda}(t_0)]_{REC} = 0$. We will retain this term, since Eq. (15) can also describe inversion recovery experiments where an inversion pulse ends at t_0.

Equation (15) takes the form of an exponential decay multiplied by $M_z^0(t)$, which is proportional to the chemical concentration function. If a way can be found to monitor $M_z^0(t)$ [or $R(t)$] over the recovery time period, then the T_1 information can be extracted with a ratio as in Eq. (14). For a radical with an absent or inaccessible center line, $M_z^0(t)$ can be obtained by summing the kinetic curves from a pair of hyperfine lines symmetrically located on either side of the center of the EPR spectrum. Such a pair of lines (which we shall call + and −) has the useful property[5] $(E_+ + E_-) = 0$, and consequently we may write

$$S_+(t-t_0) + S_-(t-t_0) = 2M_z^0(t)C(t,\tau). \quad (16)$$

It will be noted that except for the factor of 2, Eq. (16) is equivalent to Eq. (13), and in systems with only a single radical present, one can use either the summing procedure or an unpolarized center line signal $[S_0(t-t_0)]$ to obtain the time dependence of $M_z^0(t)$.

By taking the ratio of Eqs. (15) and (16) we obtain

$$\frac{S_{REF}(t-t_0) - S_{REC}(t-t_0)}{S_+(t-t_0) + S_-(t-t_0)} = \frac{1}{2}\Delta P_{z\lambda}(t_0)\exp\{-(t-t_0)/T_1\}. \quad (17)$$

Evaluation of T_1 may be accomplished by performing the point-by-point subtraction, addition, and ratio of experimental curves implied by Eq. (17), and then fitting the result of the manipulations to an exponential decay. Fitting the data in this way also allows one to determine $\Delta P_{z\lambda}(t_0)$, which is the difference in initial polarization between the reference and recovery curves. In a saturation recovery experiment, $\Delta P_{z\lambda}(t_0) = [P_{z\lambda}(t_0)]_{REF}$, whereas in an inversion recovery experiment, $\Delta P_{z\lambda}(t_0) \simeq 2[P_{z\lambda}(t_0)]_{REF}$. Consequently, the polarization at any time t_0 may be determined by beginning a dynamic polarization recovery experiment at t_0.

It should be emphasized that the subtraction/normalization procedure just outlined is very general, and can be applied to any pair of recovery and reference curves regardless of $P_{z\lambda}(t_0)$, as long as $R(t)$ is the same in both the recovery and reference experiments. We have found that the procedure gives the same result when inversion pulses, saturation pulses, or arbitrary perturbation pulses are used to generate the recovery curve. Similarly, we have found equivalent results using either $[S_+(t) + S_-(t)]$ or $S_0(t)$ in the denominator of Eq. (17).

It must also be emphasized that the ratio techniques introduced above will give a proper measure of T_1 only when $T_1^{-1} \gg k_{ex}R(t)$. Although we have used Eq. (9) to describe the polarization in the interval between perturbation and probe pulses, the description is not strictly valid immediately following a perturbation pulse since $\overline{P} \neq 1$ as was assumed in the derivation. This consideration is unimportant as long as exchange is negligible. Empirically, one can determine whether a system satisfies this condition by perturbing the system at several different times t_0 after the radical generation pulse so that $R(t_0)$ is changed over a factor of 2 or 3 in different recovery curves. If the measured recovery time remains constant, one can be certain that T_1 has been properly measured at least to within the random error limits of the experiment. These methods are illustrated below in Sec. IV.

Up to this point in our discussion of the dynamic polarization recovery experiment, we have relied on a number of simplifying assumptions, which may not be satisfied in some experiments. The equations presented above presume the creation of a single free radical species with uniform concentration throughout the sample volume. In addition, we have assumed that the signal obtained by FID integration is directly proportional to the longitudinal magnetization at the time of application of a short probe pulse. The following section will be devoted to the latter assumption, which has not been addressed in earlier publications.[7,8] The final Theory section will demonstrate that the dynamic polarization recovery method is largely insensitive to sample inhomogeneity and will indicate how the method may be extended to multiple-radical systems.

D. Polarization behavior during microwave pulses

We are interested in the transient response of the polarization to a resonant microwave field of amplitude $\omega_1 (= \gamma B_1)$ when it is applied as a pulse of duration t_p along the x axis of the rotating frame. This is a standard problem in magnetic resonance, of course, and was first solved in detail by Torrey[34] for the case of static samples. In the systems under study here, one must also consider the effects of fast chemical decay, CIDEP, and Heisenberg exchange.[7,8,11] In particular, we wish to understand how these additional effects modify the techniques of T_1 measurement in which either saturation or 180° pulses are used to perturb the spins, and 90° pulses are used to probe the recovering polarization.

It was noted in Sec. II C that a dynamic polarization recovery experiment may be interpreted in terms of a single unimolecular time constant only in the limit that Heisenberg exchange (a bimolecular process) is negligible during the period when the pulses are applied. The effects of exchange may in principle always be made negligible, albeit at the expense of sensitivity, by carrying out T_1 measurements at sufficiently low radical concentrations. This condition will be assumed in the present discussion, since dropping the ex-

change term decouples the equations for the individual hyperfine components, and enormously simplifies the analysis.

A previous publication from this laboratory[7] considered the effect of CIDEP and chemical reaction on spin-echo generation in liquids, and the same basic approach will be followed here.

If we omit the Heisenberg exchange term, Eq. (5) may be recast in matrix form as follows[7]:

$$\dot{\mathbf{P}} + [\mathbf{\Gamma} + \mathbf{\beta}]\mathbf{P} = \boldsymbol{\alpha}(t), \tag{18}$$

where

$$\mathbf{\Gamma} = \begin{bmatrix} T_2^{-1} & 0 & 0 \\ 0 & T_2^{-1} & 0 \\ 0 & 0 & T_1^{-1} \end{bmatrix},$$

$$\mathbf{\beta} = \begin{bmatrix} 0 & -\Delta\omega & 0 \\ \Delta\omega & 0 & -\omega_1 \\ 0 & \omega_1 & 0 \end{bmatrix},$$

$$\boldsymbol{\alpha}(t) = \begin{bmatrix} 0 \\ 0 \\ A(t) \end{bmatrix}, \quad A(t) = T_1^{-1} + E_\lambda k_r R(t).$$

The sign convention used here defines $\Delta\omega = \omega_0 - \omega$, where ω is the microwave frequency and ω_0 is the resonance frequency of the transition. Following the normal procedure, we have assumed that ω_1 is constant for the duration of the pulse. In practice this is a poor approximation for short microwave pulses, but the essential result should not differ as long as pulse shapes are reproducible throughout an experiment.

The general solution of Eq. (18) is of the form [35]

$$\mathbf{P}(t_p) = \mathsf{U}(t_p,0)\mathbf{P}(0) + \int_0^{t_p} \mathsf{U}(t,t')\mathbf{A}(t')dt', \tag{19}$$

where the time-dependent tensor $\mathsf{U}(t,t')$ is the solution of the homogeneous equation $\alpha(t) = \mathbf{0}$. We have defined $t = 0$ at the beginning of the microwave pulse, which has duration t_p. Following Jaynes,[35] we will make the assumption $T_2 = T_1 = T_e$, which is true for most of the small free radicals under study. With this assumption, one obtains

$$\mathsf{U}(t,t') = \exp\{-(t-t')/T_e\}\mathsf{R}(t,t'), \tag{20}$$

where

$$\mathsf{R}(t,t') = 1 - \frac{\sin b(t-t')}{b}\mathbf{\beta} + \frac{1-\cos b(t-t')}{b^2}\mathbf{\beta}^2$$

and $b = [(\Delta\omega)^2 + \omega_1^2]^{1/2}$. At this point, the desired solution for $\mathbf{P}(t_p)$ may be written in integral form, given an arbitrary boundary condition $\mathbf{P}(0)$ at the beginning of the pulse. We have

$$P_x = \left(\left[1 - \left(\frac{\Delta\omega}{b}\right)^2(1-\cos bt_p)\right]P_x(0) + \left(\frac{\Delta\omega}{b}\right)(\sin bt_p)P_y(0) + \left(\frac{\omega_1\Delta\omega}{b^2}\right)(1-\cos bt_p)\,P_z(0) + \left(\frac{\omega_1\Delta\omega}{b^2}\right)\Pi_x\right)\exp\{-t_p/T_e\}, \tag{21a}$$

$$P_y = \left(-\left(\frac{\Delta\omega}{b}\right)(\sin bt_p)\,P_x(0) + (\cos bt_p)\,P_y(0) + \left(\frac{\omega_1}{b}\right)(\sin bt_p)\,P_z(0) + \left(\frac{\omega_1}{b}\right)\Pi_y\right)\exp\{-t_p/T_e\}, \tag{21b}$$

$$P_z = \left(\left(\frac{\omega_1\Delta\omega}{b^2}\right)(1-\cos bt_p)P_x(0) - \left(\frac{\omega_1}{b}\right)(\sin bt_p)\,P_y(0) + \left[1 - \left(\frac{\omega_1}{b}\right)^2(1-\cos bt_p)\right]P_z(0) + \left(\frac{\omega_1}{b}\right)^2\Pi_z\right) \times \exp\{-t_p/T_e\} + V_\lambda, \tag{21c}$$

where

$$V_\lambda = \int_0^{t_p} \exp\{-(t_p - t')/T_e\}\,A(t')dt',$$

$$\Pi_x = \Pi_z = \Pi_{x,z} = \int_0^{t_p} \exp\{t'/T_e\}[1-\cos b(t_p - t')]A(t')dt',$$

and

$$\Pi_y = \int_0^{t_p} \exp\{t'/T_e\}\,[\sin b(t_p - t')]\,A(t')dt'.$$

The first three terms on the right of Eqs. (21a)–(21c) describe the zero-order response of an ideal system, in which the magnetization vector is tipped through an angle bt_p and the amplitude of the vector $\mathbf{P}(t_p)$ is directly proportional to the amplitude of $\mathbf{P}(0)$. The integral V_λ represents the growth of RPM CIDEP and equilibrium polarization during the pulse and is independent of the microwave field. The integrals $\Pi_{x,z}$ and Π_y represent the convolution of relaxation and CIDEP effects with the action of the microwave pulse. Obviously, in the limit of very short pulses ($t_p \to 0$), V_λ, $\Pi_{x,z}$, and Π_y will be negligible compared to the "ideal" result. It is in this limit that Eq. (6) is valid. We will now consider at what point this approximation breaks down.

The detection method used in this study is based on integration of a portion of the FID which follows a short probe pulse (Fig. 1). Optimum time resolution is obtained by sampling the FID signal with a short gate as close to the end of the probe pulse (i.e., start of the FID) as is experimentally possible. Under these conditions, the signal is proportional to the y magnetization at the end of the probe pulse, and for a probe pulse of length t_p applied at time t we have $S(t) \propto M_y(t+t_p) = M_z^0(t+t_p)P_y(t+t_p)$. The ideal experiment represented by Eq. (6) requires, in addition, that $M_z^0(t) \simeq M_z^0(t+t_p)$ and that $P_y(t+t_p) \propto P_z(t)$.

Given the signal-to-noise ratio typically encountered in these experiments, we may consider a probe pulse to be sufficiently "ideal" if it satisfies the proportionality condition $P_y(t_p) \propto P_z(0)$ to within $\pm 5\%$. For $P_x(0) = P_y(0) \simeq 0$ and $P_z(0) \sim 1$, this condition will be satisfied as long as $|\Pi_y(t_p)| \leqslant 0.05$. A similar criterion for the ideality of 180° and saturation pulses might be $|\Pi_z(t_p)| \leqslant 0.05$. However, in inversion or saturation recovery experiments where FID integration is used as a probe, it is more important to ensure that the FID signal following the probe pulse is not affected by any transverse magnetization generated by the inversion or saturation pulse. Assuming the experiment is performed approximately on resonance, one generally has $|(\Delta\omega/b)P_x(0)| \ll |(\omega/b)P_z(0)|$ so that the contribution of initial x magnetization is negligible. For pure 90° probe pulses (defined by bt_p

$= \pi/2$) the coefficient of $P_y(0)$ in Eq. (21b) is identically zero, and there would be no distortion of a polarization recovery signal due to imperfect inversion or saturation pulses. However, it is difficult to set probe pulse tip angles more accurately than $90° \pm 20°$, and as a practical matter, one should require $P_y(0) \leqslant 0.15$ to ensure the approximate proportionality between $P_y(t_p)$ and $P_z(0)$. Consequently, we shall consider 180° or saturation pulses "ideal" so long as $P_y(t_{180})$ or $P_y(t_{sat})$ is less than 0.15, even if complete inversion or saturation is not attained.

Rather than attempting solution of the integrals $\Pi_{x,z}$ and Π_y for an assumed functional form of $R(t')$, we note that the probe and inversion pulses used in our experiment are typically on the order of 100 ns in duration, and shorter pulses are quite feasible. On the other hand, the shortest second-order chemical half-lives which we can generate in our apparatus are on the order of 1 μs, and in the concentration range which this implies ($\sim 10^{-3}$ M), Heisenberg exchange is quite important.[11] Consequently, for free radical concentrations where Eqs. (21a)–(21c) can be considered valid, $A(t')$ is nearly constant over pulse intervals corresponding to probe or inversion pulses. (Note that this argument would have to exclude the presence of a fast first-order decrease of concentration.) $A(t')$ may therefore be factored out of the integrals to give upon integration

$$\Pi_y \simeq \frac{A(0)T_e^2}{1+b^2T_e^2}\left[b \cdot \exp(t_p/T_e) - \frac{\sin bt_p}{T_e} - b \cdot \cos bt_p\right] \tag{22a}$$

and

$$\Pi_{x,z} \simeq \frac{-A(0)T_e^2}{1+b^2T_e^2}\left[\frac{\exp(t_p/T_e)}{T_e} + b \cdot \sin bt_p - \frac{\cos bt_p}{T_e}\right] + A(0)T_e(\exp\{t_p/T_e\} - 1). \tag{22b}$$

Except for the inclusion of CIDEP in the factor $A(0)$, Eqs. (21) and (22) are identical to the solution of the Bloch equations obtained by other workers[36] for static samples $[A(0) \to 1/T_e]$.

Consider now the case where $t_p \ll T_e$, which one generally hopes to attain in a pulsed magnetic resonance experiment. By definition, 90° and 180° pulses correspond to the conditions $bt_p = \pi/2$ and $bt_p = \pi$, respectively. With these substitutions and approximations one obtains from Eqs. (22a) and (22b),

$$\Pi_y(t_{90}) \simeq \frac{2t_{90}}{\pi} A(0), \tag{23a}$$

$$\Pi_y(t_{180}) \simeq \frac{2t_{180}}{\pi} A(0), \tag{23b}$$

and

$$\Pi_z(t_{180}) \simeq \frac{-2t_{180}^2}{\pi^2 T_e} A(0). \tag{23c}$$

Based on Eq. (23a), a 90° probe pulse of 100 ns duration will satisfy the proportionality criterion established earlier if $|A(0)| \leqslant 7.8 \times 10^5\ s^{-1}$. This condition generally holds for hyperfine lines which are not enhanced, i.e., the center line of a radical spectrum which will be characterized by $E_\lambda = 0$. However, a more typical hyperfine line might be characterized by $T_e \simeq 2 \times 10^{-6}$ s and $|E_\lambda| \sim 25$, and in this example, the proportionality breaks down if the second-order reaction half-life $T_c = [2k_r R(0)]^{-1}$ is shorter than about 100 μs. Similarly, in a sample with $T_c < 30\,\mu$s, canonical 180° pulses ($bt_p = \pi$) can give a significant FID which may interfere with the probe pulse. Ideal inversion pulses (inverted z polarization, no FID) may still be obtained, however, by slightly adjusting the pulse width to meet the condition $(\sin bt_p)P_z(0) \simeq -\Pi_y(t_p)$.

In a number of free radical systems which we have examined, the condition $t_p \ll T_e$ cannot be obtained with present EPR equipment, and the deviation from ideality can be severe even in the absence of CIDEP. In the limit that $t_{90} = T_e$ (actually met in the case of $\cdot CH_2O^-$), one has $\Pi_y(t_{90}) \simeq T_e A(0) \sim 1$, which represents an extreme departure from the proportionality requirements for Eq. (6). $P_y(t_{180})$ may easily be greater than 0.15 in this limit, and inversion recovery experiments become extremely difficult. It is possible to obtain T_1 information in this fast relaxation regime, however, as will be demonstrated in Sec. II E.

To conclude our discussion of polarization during microwave pulses, we consider the case $t_p \gg T_e$ which corresponds to a saturating pulse. In this limit, the leading terms of Eqs. (21a)–(21c) are damped out and only the nonoscillatory terms of $\Pi_{x,z}$, Π_y, and V_λ remain. Naturally, the assumption $A(t') = \text{const}$ is no longer valid in general, but the qualitative features of the solution will not change if the assumption is retained. Equations (21a)–(21c) then reduce to the steady-state solution of Eq. (18), and one can easily remove the restriction that $T_1 = T_2$:

$$P_x(\text{sat}) = \frac{[T_1 A(t)]\omega_1 \Delta\omega T_2^2}{1 + \omega_1^2 T_1 T_2 + \Delta\omega^2 T_2^2}, \tag{24a}$$

$$P_y(\text{sat}) = \frac{[T_1 A(t)]\omega_1 T_2}{1 + \omega_1^2 T_1 T_2 + \Delta\omega^2 T_2^2}, \tag{24b}$$

$$P_z(\text{sat}) = \frac{[T_1 A(t)](1 + \Delta\omega^2 T_2^2)}{1 + \omega_1^2 T_1 T_2 + \Delta\omega^2 T_2^2}. \tag{24c}$$

Assuming that the experiment is performed on resonance ($\Delta\omega = 0$) and that $\omega_1^2 T_1 T_2 \gg 1$ as required for static saturation recovery experiments, our criterion for "ideal" saturation pulses with negligible FID yields the requirement that $|A(t)| \leqslant 0.15\,\omega_1$. In the typical experiment described above, with $T_1 = T_2 = 2\,\mu$s, $E_\lambda = 25$, and $t_{90} = 100$ ns, the ideal saturation condition will be achieved only for $T_c \geqslant 17$ μs. [Note that with these parameters inserted into Eq. (24c), the relative z polarization is only 2.4×10^{-3}.] As for the case of short pulses, ideality breaks down further as T_1 and T_2 approach t_{90}, and in the limit $t_{90} = T_1$, a saturation condition cannot be obtained.

In summary, we have shown that the FID integration method for detecting z magnetization gives a signal which is directly proportional to the polarization for sufficiently short pulses ($t_p \ll T_e$) and for sufficiently small radical pair mechanism CIDEP enhancements. A more general expres-

sion relating the FID signal to the z magnetization is needed to describe experiments where $t_p \sim T_e$ or where moderately large enhancements are present. In the following section we shall develop such an expression and consider the effects of nonideal pulses and samples on the basic dynamic polarization recovery method.

E. Dynamic polarization recovery in nonideal systems

The dynamic polarization recovery method proposed in Sec. II C relied on a number of assumptions which are often not satisfied in pulsed experiments. Most notably, it was assumed that a single free radical species could be generated, and that the system could be characterized by a uniform concentration $R(t)$. While the first of these assumptions can be met by careful choice of the experimental conditions, the second condition is difficult to achieve because typical laser and electron beams used to generate free radicals are nonuniform. This leads to concentration gradients in the sample which seriously affect the experiment when the kinetics are dominated by second-order processes. A further assumption made earlier involved the nature of the signal detected by FID integration. As was shown in the previous section, many of our experiments were performed in a regime where Eq. (6) cannot be considered valid.

The purpose of this section is to consider in detail how a breakdown in any of these assumptions might change the measured recovery time. We will consider each assumption in turn to develop more rigorous analogs of the expressions presented in Sec. II C. Surprisingly, many of the nonidealities which seriously affect the raw data tend to cancel out when the subtraction and ratio operations are performed. Because of this, the simple expressions presented in Sec. II C are entirely adequate for understanding the experiments reported in Secs. III and IV of this paper.

1. Nonideal microwave pulses

As was noted in the previous section, the signal detected by FID integration after a short probe pulse is proportional to the y magnetization present at the end of the pulse. For a probe pulse of length t_p applied at time t we have

$$M_y(t+t_p) = M_z^0(t+t_p)\,[a_x(t_p)P_x(t) + a_y(t_p)P_y(t) + a_z(t_p)P_z(t) + a_\pi(t_p)\Pi_y(t,t_p)]\,, \tag{25}$$

where the coefficients $a_i(t_p)$ may be obtained by inspection of Eq. (21b). $P_x(t)$ and $P_y(t)$ will be zero in a single-pulse experiment (reference curve), and in a two-pulse experiment (recovery curve) the coefficients $a_x(t_p)$ and $a_y(t_p)$ can be made negligible by careful adjustment of the pulse widths. In either case, the first two terms of Eq. (25) can be ignored and for a fixed probe pulse length the signal will be of the form

$$S(t) \propto M_z^0(t) \times \Big(P_{z\lambda}(t) + \epsilon(t_p)\Big[T_1^{-1} + E_\lambda k_r R(t)\Big] C(t,\tau)\Big), \tag{26}$$

where all of the pulse width dependent terms have been grouped in $\epsilon(t_p)$ and Π_y has been expanded using Eq. (22a) and the definition of $A(t)$.

Consider now the dynamic saturation recovery experiment proposed in Sec. II C 2. If we use Eq. (26) instead of Eq. (6), the recovery signal for a center line ($E_\lambda = 0$) corresponding to Eq. (12) is of the form

$$S_{\rm REC}(t-t_0) = M_z^0(t)[1 - \exp\{(t-t_0)/T_1\} + \epsilon/T_1]C(t,\tau) \tag{27}$$

and the reference signal is given by

$$S_{\rm REF}(t-t_0) = M_z^0(t)\,[1 + \epsilon/T_1]C(t,\tau). \tag{28}$$

The ratio of these two expressions reduces to Eq. (14) as long as $\epsilon/T_1 \ll 1$, which should always be true in experiments where a significant degree of saturation can be achieved. It should be noted that the reference signal from an unpolarized line [Eq. (28)] is directly proportional to $M_z^0(t)$ regardless of the correction term ϵ/T_1. This means that the center line signal accurately tracks the chemical concentration even when $t_p \geqslant T_1$.

The more general subtraction/normalization procedure introduced in Sec. II C 3 works on polarized lines and automatically corrects for pulse imperfections. When the difference between reference and recovery curves is calculated, the correction terms involving $\epsilon(t_p)$ subtract out, giving a result identical to Eq. (15). Addition of the signals from oppositely polarized lines results in cancellation of all terms involving E_λ, and leaves an expression similar to Eq. (16). Finally, the ratio of these expressions gives

$$\frac{S_{\rm REF}(t-t_0) - S_{\rm REC}(t-t_0)}{S_+(t-t_0) + S_-(t-t_0)} = \frac{\Delta P_{z\lambda}(t_0)\exp\{-(t-t_0)/T_1\}}{2(1+\epsilon/T_1)}\,, \tag{29}$$

which has the same functional form as Eq. (17), but a slightly different intercept at $t = t_0$.

2. Nonuniform samples

In most pulsed experiments, transients are created with nonuniform photon or electron beams, and the sample under observation may contain significant concentration gradients. This effect may be accounted for by integrating Eq. (26) over the entire sample volume as follows:

$$S(t) = \int_v d\mathbf{r} M_z^0(t,\mathbf{r})\Big(P_{z\lambda}(t,\mathbf{r}) + \epsilon(t_p) \times [T_1^{-1} + E_\lambda k_r R(t,\mathbf{r})]\Big) C(t,\tau,\mathbf{r}). \tag{30}$$

In this expression, the vector $\mathbf{r}$ denotes position in the sample, and we have assumed that the EPR cavity is equally sensitive to all parts of the sample.

One can now develop expressions similar to Eqs. (14) and (17) which reflect the sample inhomogeneity. For a nonpolarized center line we have

$$\frac{S_{\rm REC}(t-t_0)}{S_{\rm REF}(t-t_0)} = \frac{1 - \exp\{-(t-t_0)/T_1\} + \epsilon/T_1}{1+\epsilon/T_1}\,, \tag{31}$$

since the integral $\int_v d\mathbf{r} M_z^0(t,\mathbf{r})C(t,\tau,\mathbf{r})$ divides out of the ratio.

For the more general subtraction/normalization procedure, we obtain

$$\frac{S_{\mathrm{REF}}(t-t_0)-S_{\mathrm{REC}}(t-t_0)}{S_+(t-t_0)+S_-(t-t_0)} = \frac{\exp\{-(t-t_0)/T_1\}}{2(1+\epsilon/T_1)}\,\overline{\Delta P(t_0)}, \tag{32}$$

where we define

$$\overline{\Delta P(t_0)} = \frac{\int_v \Delta P(t_0,\mathbf{r}) M_z^0(t,\mathbf{r}) C(t,\tau,\mathbf{r})}{\int_v d\mathbf{r} M_z^0(t,\mathbf{r}) C(t,\tau,\mathbf{r})}.$$

This expression is very similar to Eq. (29), except that the coefficient $\overline{\Delta P(t_0)}$ is, in general, time dependent. However, as long as the concentration gradients in the sample are not severe, $\overline{\Delta P(t_0)}$ is a very weak function of time, and we have found that it may usually be treated as a constant.

3. Extension to multiple-radical systems

The derivation of Eqs. (11) and (21a)–(21c) relied on the central postulate that the sample contains only a single free radical species. If this requirement is relaxed, Eq. (7) must be rewritten in the form

$$\dot{P}_{z\lambda} = \frac{-(P_{z\lambda}-1)}{T_{l\lambda}} - \sum_{\mu=1}^{N} k_{\lambda\mu}\left[R_\lambda(t)P_{z\lambda} - R_\mu(t)P_{z\mu}\right] + \sum_{\mu=1}^{N} E_{\lambda\mu}(k_r)_{\lambda\mu}R_\mu(t), \tag{33}$$

where we now sum over N different hyperfine components, which may arise from chemically different species and exhibit quite different reactivity and relaxation behavior than the radical of interest. By analogy with Eq. (7), one can see that the solution of Eq. (33) will be of the general form

$$P_{z\lambda}(t) = 1 + [P_{z\lambda}(t_0)-1]\exp\left[-\frac{(t-t_0)}{T_{1\lambda}} - H_\lambda(t)\right] + V_\lambda(t), \tag{34}$$

where $H_\lambda(t)$ includes the relaxation effects of Heisenberg exchange and $V_\lambda(t)$ represents the combined RPM CIDEP enhancement effects from all radicals present. Consequently, the difference between a polarization recovery curve and a reference curve will again lead to a function of the form (omitting integration over the sample volume)

$$[S_{\mathrm{REF}} - S_{\mathrm{REC}}] = M_{z\lambda}^0(t)\Delta P_{z\lambda}(t_0) \times \exp\left[-\frac{(t-t_0)}{T_{1\lambda}} - H_\lambda(t)\right] C(t,\tau). \tag{35}$$

In the limit of sufficiently low concentrations, $H_\lambda(t_0)$ can always be made negligible relative to T_1^{-1}. It will therefore be possible to extract $T_{1\lambda}$ using the ratio methods of Sec. II C if $M_{z\lambda}^0(t)$ is nearly constant over the recovery time period, or if some other means can be found to measure $M_{z\lambda}^0(t)$. As long as there is no net effect CIDEP, $M_{z\lambda}^0(t)$ can be synthesized from the sum of a pair of curves $S_+(t-t_0)$ and $S_-(t-t_0)$ as before. This situation may arise if all of the radicals in the system have nearly the same g factor or if the rates for cross reactions are relatively low. If net effect CIDEP is significant, then the chemical concentration of the species of interest may still be followed by other techniques, such as optical absorption or laser-induced fluorescence.

F. Summary

In summary, we have proposed a simple procedure for extracting T_1 information from pulsed EPR experiments, which avoids reliance on multiple-parameter least-squares analysis of systems whose EPR spectra may be complicated by fast chemical decay and CIDEP. The method is self-calibrating in the sense that no detailed information is needed about the microwave power at the sample. Our analysis has shown that the procedure will give the correct T_1 result regardless of the details of chemical decay of the sample, which may result from several competing reactions. The method is also largely immune to any concentration gradients which may affect the kinetics. The primary experimental requirements are that free radical concentrations be low enough to avoid distortion of the polarization recovery signal by Heisenberg exchange, and that the free radicals be produced in reproducible pulses so that signal-averaging techniques may be used.

Sections III and IV of this paper will describe dynamic polarization experiments which were analyzed using the methods described above. In Sec. V, the implications of these experiments are discussed, and opportunities for future experiments using these techniques will be pointed out in Sec. VI.

III. EXPERIMENTAL

Free radicals were generated in N_2O-saturated aqueous solution by pulse radiolysis with 3 MeV electrons from a Van de Graaff accelerator. The primary products of the radiolysis [$^{\cdot}OH$ or $^{\cdot}O^-$, $^{\cdot}H$, $(e^-)_{aq}$][37] were used to generate most of the secondary radicals of interest by the following series of reactions[38–40]:

$$H^{\cdot} + OH^- \rightarrow (e^-)_{aq} + H_2O, \tag{R1}$$

$$(e^-)_{aq} + N_2O \rightarrow N_2 + {}^{\cdot}O^-, \tag{R2}$$

$${}^{\cdot}O^-({}^{\cdot}OH) + RH \rightarrow R^{\cdot} + OH^-(H_2O). \tag{R3}$$

Exceptions to this scheme are $\cdot SO_3^-$, in which the radical is formed by the electron transfer (R4),[41]

$$SO_3^{=} + {}^{\cdot}O^- \rightarrow {}^{\cdot}SO_3^- + 2OH^- \tag{R4}$$

and $\cdot CH_3$, which is formed by addition of $^{\cdot}O^-$ to DMSO[42]:

$$(CH_3)_2SO + {}^{\cdot}O^- \rightarrow CH_3SO_2^- + \cdot CH_3. \tag{R5}$$

In general, the radical precursor RH was introduced in 0.1–0.5 M concentration both to increase the rate of reaction (R3) and to make possible several hours of signal averaging with the same sample before product buildup became significant. In most cases, the solutions were run at pH = 14 (1.0 M NaOH) to increase the rate of reaction (R1). Under these conditions, reactions (R1)–(R5) run to completion within about 200 ns after the radiolysis pulse. Hydroxyalkyl radicals were also studied at pH = 7 or lower, both in a 0.5 M phosphate buffer and in D_2O. Under these conditions, both H$^{\cdot}$(D$^{\cdot}$) and hydroxyl react with the alcohol by hydrogen

abstraction, and reaction (R6) takes the place of reaction (R1)[38]:

$$H^{\cdot} + HROH \rightarrow {}^{\cdot}ROH + H_2. \quad (R6)$$

Except in the case of MeOH, reaction (R6) is also complete in well under 200 ns.

All of the radical precursors used in this study were small molecules chosen to give predominantly one product by reactions (R3)–(R7). These radicals, once created, disappear almost exclusively by second-order combination or disproportionation processes with rates on the order of 10^9 $M^{-1}\,s^{-1}$.[43] Because high concentrations (10^{-4}–10^{-3} M) of free radicals were generated, side reactions with small amounts of impurities were not important on the (0–100 μs) time scale of interest. Consequently, reagent grade chemicals were used throughout with no additional purification.

Viscosity measurements of some sample solutions were made with an Ostwald viscometer calibrated using water, methanol, and ethanol at 20 °C. Density measurements were made by pycnometry using 1.000 ml of solution. Viscosity of the solutions irradiated in the EPR experiments was not measured directly, but no significant change in viscosity upon irradiation is expected due to the relatively small amounts of product formed.

The radiolysis was performed *in situ* in the EPR cavity, introducing the sample as a free-flowing liquid jet.[44] Approximately 1 ℓ of solution was continuously recirculated and bubbled with N_2O using the system diagrammed in Fig.2. The sample reservoir is a 1 m long, 2 in. diam column partially filled with glass beads to increase the available surface area for gas–liquid equilibration. This arrangement serves the dual purpose of keeping the solution saturated with N_2O (introduced at the bottom) and removing oxygen which becomes dissolved in the solution through contact with the atmosphere in the cavity. In most cases, the possibility of O_2 contamination was further reduced by using an N_2O atmosphere in the cavity. The temperature and *p*H of the solution were monitored continuously by a thermocouple and *p*H electrode inserted into the sample stream above the jet.

The pulsed EPR spectrometer used in this study has been described in previous publications.[7,8] No changes have been made in the pulsed microwave detection system. A PDP 11/23-Plus minicomputer now digitizes the signal from the Model 162 PAR boxcar integrator, and selects both the digital time delays and the magnetic field settings. Data are transferred to a VAX-11 computer for analysis.

The basic pulse sequence used for the polarization recovery measurements was shown in Fig. 1. The electron pulses used to create free radicals were typically 200–300 ns in duration. Following the electron pulse, either a 200 ns microwave inversion pulse or a 1–10 μs saturation pulse was applied to the sample. Inversion pulse widths were adjusted to find a zero in the FID amplitude observed on an oscilloscope, whereas saturation pulse durations were selected by multiplying the observed FID decay time (T_2^*) by 10. (When short saturation pulses were needed in order to probe the sample at short times after the radiolysis pulse, T_2^* was reduced by spoiling the field homogeneity.[7]) At a variable time delay after the perturbation pulse, a probe pulse of 60–100 ns

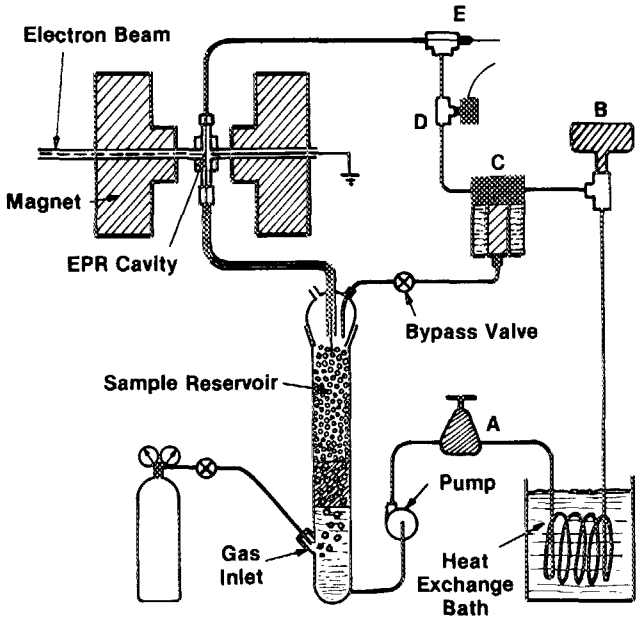

FIG. 2. Schematic diagram of the liquid jet flow system. The sample reservoir is a glass tube partially filled with glass beads to improve the efficiency of saturation with N_2O, which is introduced at the bottom of the column. Pressure fluctuations introduced by the pump are controlled by a Cash-Acme type G-60 pressure regulator (A) and a modified Tyler Pipe Corp. water "hammer arrestor" (B). Any small particulate matter in the sample is removed by a Balston Co. grade DX filter (C). Pressure at the capillary entrance above the cavity is adjusted with the bypass valve and monitored with an electronic pressure transducer (D). When *p*H needs to be monitored, the pressure transducer is replaced by a *p*H electrode. The temperature of the solution is controlled with the heat exchange bath and continuously monitored by a thermocouple inserted into the flow stream (E). A vertical free-standing liquid jet is formed in the cavity after the solution flows through a 2.2 mm diam capillary. Gravity flow returns the sample to the reservoir. The conditions necessary for obtaining liquid jets suitable for EPR spectroscopy were discussed in an earlier publication (Ref. 44).

duration was applied and the initial amplitude of the resulting free induction decay signal was sampled with a 50 ns boxcar gate. The recovery of the magnetization was tracked by incrementing the time delay between the probe pulse and the saturation or inversion, pulse. The recovery curve was compared with a similar reference experiment in which the perturbation pulse was absent.

In addition to the signals from transient radicals, we often observe a static background signal from paramagnetic impurities adsorbed on the cavity walls, and it is necessary to subtract a base line curve from the saturation recovery curves. To increase efficiency of data collection and simultaneously check for the effects of Heisenberg exchange, one base line curve and several (usually three) saturation recovery curves, each consisting of 50–60 time delay points, are collected in a single "sweep." The base line curve is collected over a time interval just before the electron pulse while the recovery curves are collected over several different time intervals following radical creation with the radiolysis pulse. These "sweeps" of several recovery curves plus base line are repeated and summed until the signal-to-noise ratio is judged acceptable. In general, between 500 and 2500 individual pulse sequences are averaged for each time delay point, and a set of several recovery curves is obtained in somewhat less than 15 min.

Immediately following the end of each polarization recovery experiment, a reference experiment was performed by setting the perturbation pulse amplitude to zero. In all other respects, the recovery and reference experiments were identical. In the case of recovery experiments on polarized lines, a second reference curve was collected from the corresponding oppositely polarized line. Generally speaking, a set of recovery and reference curves could be obtained in less than half an hour, with overall signal-to-noise ratio greater than 10.

A significant fraction of the noise from our dc-coupled detection electronics is low frequency power line pickup which appears as a pulse-to-pulse base line "jitter" on the shorter time scale of the FID signal. We eliminated this noise contribution by triggering the experiment on a convenient harmonic of the line frequency (usually 360 Hz) and summing the signal over an integral number of line periods before reading and resetting the boxcar averager. This effectively eliminates "base line" noise in the same way as triggering at the line frequency, but allows for signal averaging rates in excess of 60 Hz.

In several experiments, the perturbation pulses were shifted in phase by 180° on alternate pulse sequences in an attempt to eliminate any contributions to the recovery signal from a FID after the first pulse. In saturation recovery experiments, no difference in the T_1 obtained with or without shifting was noticed, although shifting considerably improved the base line linearity by eliminating most of the static background signal. Unfortunately, the diode phase shifter available for the experiment had the unwanted side effect of attenuating the phase-shifted pulse by 10%–20%, which changed the effective tip angle of the microwave pulses. Consequently, phase shifting was not attempted in inversion-type experiments, where good 180° pulses were desired.

Due to the rise time and recovery characteristics of the microwave switches, the shortest useful delay between satu-

TABLE I. Compilation of T_1 measurements for various free radicals generated in aqueous solution. Measurements were typically performed on the $m = 0$ hyperfine component or on the pair of lines with the smallest splittings relative to the center. Temperature and pH of the sample solutions were monitored during experiments. Viscosities were measured separately at 20 °C and are presented for qualitative comparison only. See text for discussion of individual radicals.

Radical	Sample solution	Viscosity[a] (cP)	Temperature pH	No. Expts averaged	T_1[b] (μs)
$\cdot SO_3^-$	0.5 M Na_2SO_3 1.0 M NaOH		14–19 °C pH = 14	14	2.0
	0.5 M Na_2SO_3 0.1 M NaOH		14–16 °C pH = 13	7	1.9
$\cdot CH_3$	0.1–0.5 M DMSO 1.0 M NaOH	1.25	19 °C pH = 14	6	0.2
$\cdot CH_2COO^-$	0.5 M NaOAc 1.0 M NaOH	1.40	17–19 °C pH = 14	40	2.0
$\cdot CH(COO^-)_2$	0.5 M Malonic Acid 2.0 M NaOH	1.68	18 °C pH = 14	2	2.9
$^-OC(COO^-)_2$	0.1 M Tartronic Acid 1.2 M NaOH		17 °C pH = 14	(3)	~3.6 $3.5 < T_1 < 4.0$
$^-OCHCOO^-$	0.1 M Tartronic Acid 1.2 M NaOH		17 °C pH = 14	6	1.4
$\cdot CH_2O^-$	0.5 M MeOH 0.1 M NaOH	1.27	10 °C pH = 13	3	~0.10 $0.08 < T_1 < 0.15$
$CH_3\dot{C}HO^-$	0.5 M EtOH 1.0 M NaOH	1.32	18 °C pH = 14	1	0.7
$(CH_3)_2\dot{C}O^-$	0.5 M iPrOH 1.0 M NaOH	1.36	16 °C pH = 14	3	1.6
$\cdot CH_2OH$	0.5–1.0 M MeOH 1.0 M Phosphate buffer	1.38	17 °C pH = 6.6–6.8	4	0.6
$CH_3\dot{C}HOH$	0.5 M EtOH 0.5 M Phosphate buffer	1.44	18 °C pH = 6.8	3	1.3
$(CH_3)_2\dot{C}OH$	0.25 M iPrOH 0.5 M Phosphate buffer	1.51	17 °C pH = 6.8	4	2.7
$\cdot CH_2OD$	0.5 M MeOH in D_2O Acidified with H_2SO_4		9 °C pD = 3.6 19 °C pD = 3.2	3 6	0.72 0.53
$(CH_3)_2\dot{C}OD$	0.5 M iPrOH in D_2O Acidified with H_2SO_4		19 °C pD = 3.5	6	2.2
	0.5 M iPrOH in D_2O 0.5 M Phosphate buffer		19 °C pD = 7.0	8	2.5

[a] Viscosity measured separately at 20 °C.

[b] One standard deviation is estimated to be 10% for all cases based on variations among replicate determinations.

ration and probe pulses was found to be approximately 200 ns. Shorter delays resulted in some perturbation of the shape and width of the probe pulse, and a corresponding change in the effective tip angle as the delay was scanned. This limited reliable measurements of recovery times to 200 ns or longer. The T_1 estimate of 100 ns for the radical $\cdot CH_2O^-$ is based on an observed FID decay time of 100 ± 20 ns and the assumption that $T_1 = T_2$. The polarization recovery time was clearly $\leqslant 150$ ns, but could not be accurately measured.

IV. RESULTS

A. General comments

The dynamic polarization recovery experiment was developed in the course of our study of radical pair CIDEP in order to provide an "independent" measurement of T_1, which is a critical parameter in relating the observed CIDEP enhancements to theory. Since T_1 exhibits a strong dependence on temperature and viscosity, it has become our practice to measure T_1 on a routine basis for each free radical in the sample mixture under study. Over several months, we have accumulated a large number of T_1 measurements on a variety of small free radicals. The results are summarized in Table I, and peculiarities of the various systems are discussed below.

Both the dynamic saturation recovery and dynamic inversion recovery methods introduced in Sec. II were used with good success. The choice of method was largely determined by the signal-to-noise ratio and the nature of the particular free radical spectrum. Whenever possible, an unpolarized center line was used to provide the "chemistry" normalization curve (S_{REF}), since this avoids some possibility of systematic error in summing two polarized reference curves. When the FID signal was large enough to be easily seen on an oscilloscope, inversion recovery was often used because the difference between recovery and reference curves (i.e., the effective signal) is about twice as large as in the saturation experiment. When signal-to-noise was poor and the inversion pulse was difficult to adjust, saturation recovery was preferred to eliminate any uncertainty due to the precise microwave pulse width needed for inversion. The two basic methods are illustrated in Figs. 3 and 4 for an unpolarized center line, and Fig. 5 shows data for a system which has all polarized lines.

The dynamic saturation recovery experiment is demonstrated for the center line of the $\cdot CH_2COO^-$ radical in Fig. 3. The upper plot shows the full FID kinetics curve following a 200 ns radiolysis pulse, with three saturation recovery curves superimposed. Base line subtraction has already been performed. As predicted by Eq. (11), the magnetization signal recovers to its unperturbed amplitude after several T_1 periods. The point-by-point ratio of $S_{REC}(t - t_0)/S_{REF}(t - t_0)$ is shown for the three saturation recovery epochs in plots I through III. A least-squares fit of each ratio to the function $A(1\text{-}\exp\{-t/T_1\})$ is indicated by the solid line. All three T_1 numbers obtained in this experiment are the same to well within one standard deviation, which indicates that Heisenberg exchange does not compete significantly with the unimolecular relaxation. The amplitude factor A is included in the fit to detect any changes in the instrument response function between the recovery and reference curves. Often small changes ($\sim 10\%$) are induced in the instrument response by the change in duty cycle of the high power traveling-wave tube (TWT) amplifier when the saturation pulse is removed. In the experiment shown in Fig. 3 the amplitude factor was very nearly unity, as expected in the ideal case.

In Fig. 4, data from a dynamic inversion recovery experiment is shown for the same (center) line of $\cdot CH_2COO^-$. Inversion was accomplished with a 200 ns microwave pulse applied at 0.1, 15.1, or 30.1 μs following the 200 ns radiolysis

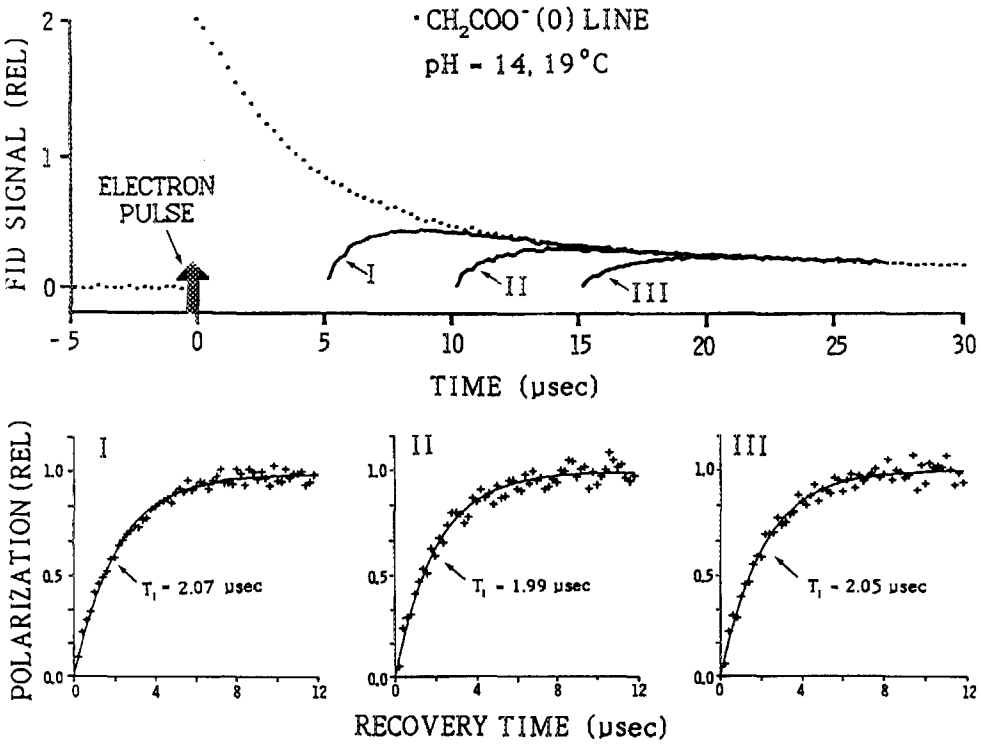

FIG. 3. Dynamic saturation recovery of $\cdot CH_2COO^-$. The upper figure shows the FID kinetics trace [$S_{REF}(t)$, dotted line] of the unpolarized center line following a 200 ns electron pulse. Superimposed are three dynamic saturation recovery curves [$S_{REC}(t)$, solid lines I, II, and III] for which the 2 μs saturating pulse ended at 5, 10, and 15 μs after the electron pulse, respectively. Each data point represents an average of 1300 individual pulse sequences. The ratios $S_{REC}(t - t_0)/S_{REF}(t - t_0)$ for the three data sets are plotted in the figures labeled I–III. The T_1 numbers indicated are calculated from a least-squares fit of the ratios (superimposed solid lines) to the function $A(1 - \exp\{-t/T_1\})$.

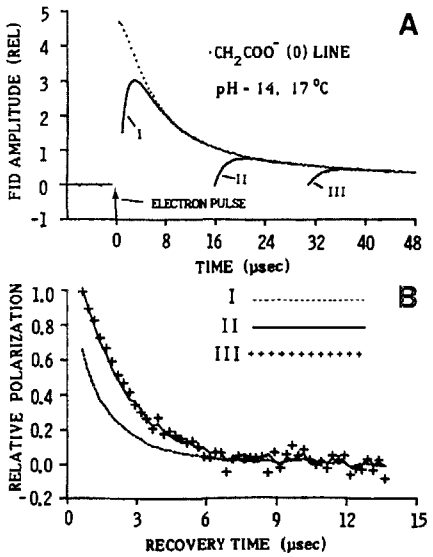

FIG. 4. Dynamic inversion recovery of $\cdot CH_2COO^-$. Plot A shows the FID kinetics trace [$S_{REF}(t)$, dotted line] of the unpolarized center line following a 200 ns electron pulse. Inversion pulses (200 ns) were applied at times 0.1, 15.1, and 30.1 μs after the electron pulse and the recovery curves [$S_{REC}(t)$, labeled I, II, and III] are superimposed on the unperturbed signal. In plot B, the ratios $[S_{REF}(t-t_0) - S_{REC}(t-t_0)]/S_{REF}(t-t_0)$ are shown for the three different time periods. The first recovery time point corresponds to a minimum delay of 400 ns between inversion and probe pulses, which was necessary to avoid problems of probe pulse distortion. The ratios for II and III superimpose and yield a T_1 value of 2.1 μs. Curve I clearly recovers much faster, which demonstrates the importance of Heisenberg exchange at the higher free radical concentration present immediately after the electron pulse.

pulse. The three recovery curves are shown superimposed on the unperturbed FID kinetics in plot A, while in plot B the results of the calculation $[S_{REF}(t-t_0) - A \cdot S_{REC}(t-t_0)]/S_{REF}(t-t_0)$ are shown. The factor A was needed to correct for a small change in the instrument response between the reference and recovery experiments, and was obtained by forcing the equality $A \cdot S_{REC}(t-t_0)/S_{REF}(t-t_0) = 1$ in the limit $(t-t_0) \sim 5T_1$. It will be noted immediately that the relative polarization curves II and III are identical to within the experimental scatter, but the recovery of curve I is much faster. The second-order half-life $T_c(t_0)$ at the beginning of curve I is roughly 2 μs, and assuming a self-combination rate constant of $10^9\ M^{-1}\ s^{-1}$ for $\cdot CH_2COO^-$ radicals,[43] one can estimate an initial concentration of 5×10^{-4} M. At this concentration, one expects that Heisenberg exchange should compete with the unimolecular relaxation processes if $T_1 \simeq 2$ μs. By the beginning of recovery curve II, the concentration has decreased by about a factor of 8, and Heisenberg exchange is no longer an important source of relaxation. This behavior is very common in our experiments, where high initial free radical concentrations are generated. The effects of exchange can always be avoided by delaying the microwave perturbation pulse sufficiently long after the radical creation pulse. Alternatively, smaller radiolysis pulses may be used, or the electron beam may be diffused over a larger sample volume to reduce the initial concentration. The advantage of performing several recovery experiments starting at various times t_0 after the radiolysis pulse as shown in Fig. 4 is that one can readily discern whether Heisenberg exchange is present by the change in apparent relaxation times.

The time resolution of our current instrumentation is illustrated in Fig. 5 by a dynamic polarization recovery experiment on the methyl radical. The FID kinetics traces for the $\cdot CH_3$ + 1/2 and − 1/2 lines following a 300 ns electron pulse are shown in plot A. Since methyl has no (unpolarized) center line, the signals from the + 1/2 and − 1/2 lines were added together to synthesize a chemistry reference curve. Saturation pulses of 1.0 μs duration ($\sim 5T_1$) were applied immediately after the radiolysis pulse and at 4.0 μs seconds delay, but as predicted in Sec. II D, complete saturation was not obtained. Saturation recovery and reference curves for both EPR lines and for both recovery periods are shown in plots B–E. Note that over recovery interval I, the − 1/2 line is polarized in emission, whereas in interval II the same line is observed in absorption. Consequently, the dynamic polarization recovery in plot D (interval I) occurs in a *negative* direction as it approaches the unperturbed reference curve, but the recovery of plot E (interval II) is in the positive direction.

Plots F–I show the ratios

$$[S_{REF}(t-t_0) - A \cdot S_{REC}(t-t_0)] / [S_+(t-t_0) + S_-(t-t_0)],$$

where the scaling factor A is determined as for the inversion recovery experiment. The solid lines show a least-squares fit of the ratios to the function $B \cdot \exp(-t/T_1)$. At recovery times $(t-t_0)$ less than ~ 100 ns, one can see a deviation from the exponential fit, which is due to distortion of the probe pulse at short time delays after the perturbation pulse. The T_1 numbers obtained in plots F–H all agree to well within experimental error. The result in plot I differs somewhat because of the very poor signal-to-noise ratio. The scaling factor B should correspond to the relative polarization of the reference curve at $t = t_0$, and the values obtained by the least-squares analysis are consistent with the relative peak heights obtained from field-swept spectra at these times after the radiolysis. This demonstrates the possibility, mentioned in Sec. II, that absolute polarization at any point of the M_z kinetics curve may be extracted by performing a dynamic saturation recovery experiment.

In Table I we have compiled T_1 results for the free radical systems studied thus far, together with a number of room temperature viscosity measurements performed on the sample mixtures. Individual T_1 determinations were characterized by a standard deviation based on the two-parameter fit to an exponential decay. The T_1 numbers reported in the table represent an average over all of the available recovery measurements, weighted by the variance of the two-parameter fit. Results for different hyperfine components of the same radical spectrum were all averaged together, since we found no differences in T_1 of different lines outside of the basic uncertainty in the measurement. Recovery curves which showed evidence of being influenced by Heisenberg exchange were not included in the average.

In general, the T_1's for the several recovery curves in a given data set agree to within the random error limits expected from the standard deviation of the fit. However, repeated determinations of T_1 on the same system ($\cdot CH_2COO^-$ was used extensively as a test case) showed variation in T_1 in

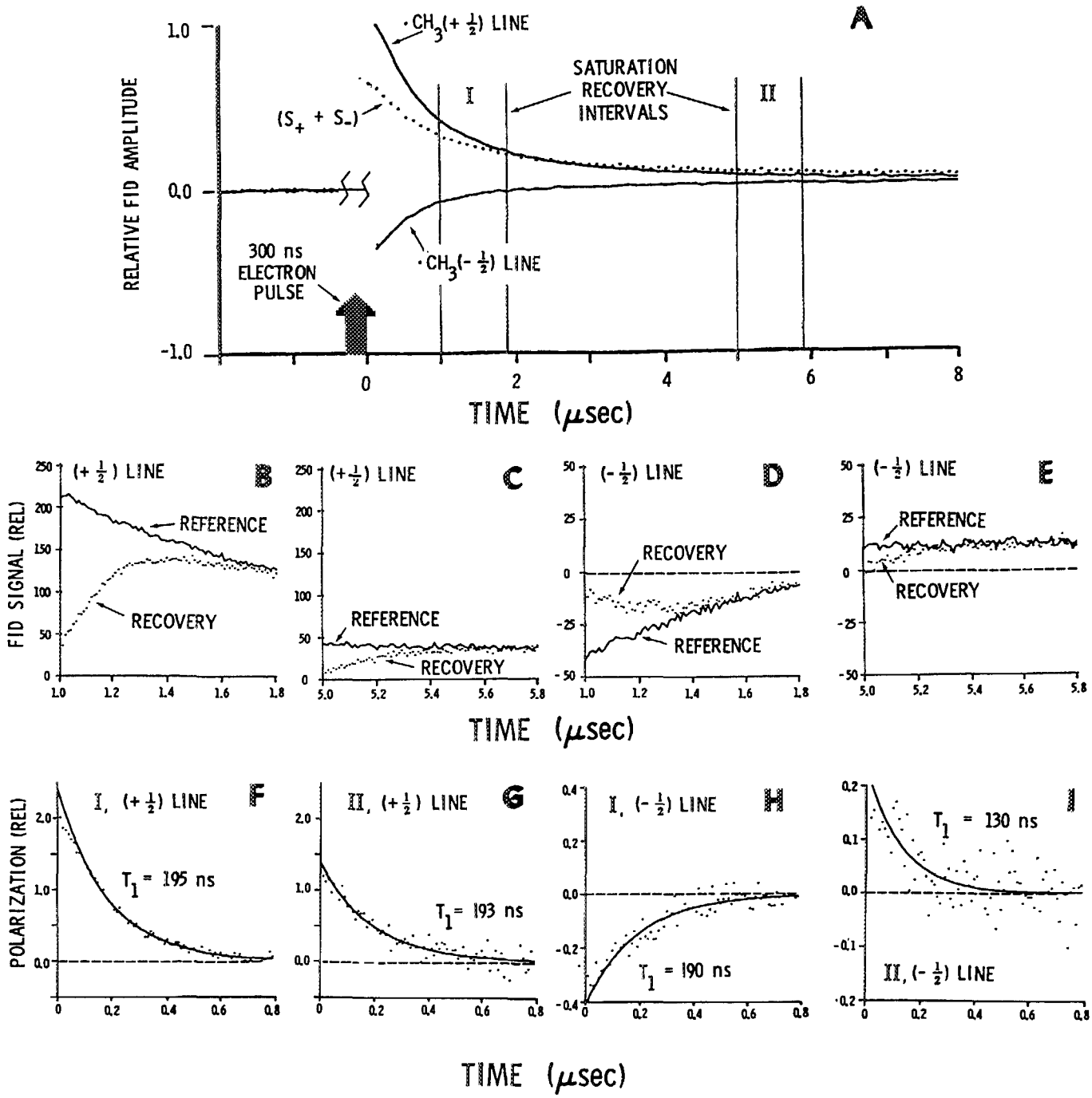

FIG. 5. Dynamic polarization recovery of the methyl radical. In plot A, the FID signal amplitude from the + 1/2 and − 1/2 lines of $\cdot CH_3$ are shown as a function of time after radical creation with a 300 ns radiolysis pulse. The dotted curve indicates the sum of + 1/2 and − 1/2 line signals, which according to theory is proportional to the chemical concentration. The initial chemical half-life is approximately 2.0 μs. Plots B–E show polarization recovery and reference curves of both lines for the time periods I and II indicated on plot A. The perturbation pulse was 1.0 μs long ($\sim 5T_1$) in all cases, but complete saturation was not obtained. The function $(S_{REF} - S_{REC})/(S_+ + S_-)$ corresponding to the raw data of B–E is plotted in F–I. The solid curves represent least-squares fits to an exponential decay function and the T_1 values so obtained are indicated. See text for discussion.

excess of the uncertainty expected from purely random noise. We believe the additional variation in measured T_1 arises because of imperfections in the base line subtraction, small changes in the spectrometer response between reference and recovery curves, and small drifts in the magnetic field during experiments. None of these error sources are reflected in the standard deviation of the fit, since the ratios of recovery and reference curves always closely resemble a single exponential decay. The total uncertainty of the subtraction/normalization method for T_1 determination seems to be characterized roughly by a 10% standard deviation, based on the large number of experiments performed on the $\cdot CH_2COO^-$ and $\cdot SO_3^-$ systems. The numbers listed in Table I may therefore be considered accurate to about ± 10%.

We wish to emphasize again that the T_1 measurements described here were performed primarily as an aid to the

analysis of effects occurring at high radical concentrations. In almost all cases, the electron beam was focused as tightly as possible to produce initially high free radical concentrations in a small volume. This experimental arrangement has the disadvantage that by the time concentrations are sufficiently low to measure T_1 in the absence of Heisenberg exchange, a large fraction of the free radical sample has decayed by second-order reaction. Improved signal-to-noise ratios in the polarization recovery experiments should be obtained in principle by defocusing the electron beam to create more free radicals in a larger sample volume with lower second-order reaction rates. We have not found it necessary to do this in the systems studied to date.

B. Carboxylic acids

The acetate radical anion $\cdot CH_2COO^-$ was used extensively as a test case in our experiments, and this is reflected by the large number of T_1 determinations indicated in Table I. Experiments were performed on all three hyperfine lines, using both inversion recovery and saturation recovery techniques. In several experiments it appeared that T_1 for the center line was slightly longer than T_1 of the outer lines, but the apparent difference was within the $\pm$ 10% uncertainty found for consecutive determinations on the same line. Any real difference is apparently at or below the 10% level in this system, and consequently we have averaged the T_1 determinations for all three hyperfine lines to obtain the 2.0 μs value shown in Table I.

Two previous publications from this laboratory have reported T_1 values for the acetate radical which differ from that obtained in the present study. In Ref. 7, a T_1 estimate of 1.4 μs was reported, based on a multiple-parameter fit of kinetic curves from the high and low field lines. A more systematic study in Ref. 11 extrapolated a unimolecular T_1 of 2.57 $\pm$ 0.03 μs. Both previous determinations were subject to significant systematic errors which have been corrected using the dynamic polarization recovery method. The previous estimates relied on curve fitting of the initial part of CIDEP kinetics curves, and at pH 10–12 this portion of the curve may have been affected by hydrogen atom chemistry at about the 10% level. More seriously, the data was analyzed with the assumption that a uniform free radical concentration was generated with the radiolysis pulse. Since the accelerator beam cross section is typically Gaussian in shape, this is a very poor approximation, and the resulting systematic error could easily account for the difference between the previous reports and the result obtained in this study.

Fessenden[13] performed progressive saturation experiments on both $\cdot CH_2COO^-$ and $\cdot CH(COO^-)_2$, and obtained T_1 values of 1.4 and 1.6 μs for the two radicals, respectively. Fessenden's experiments were performed in dilute aqueous solution (viscosity probably $\sim$1 cP), whereas our measurements have been made in more concentrated solutions which have greater viscosity. The disparity between his results and ours may be substantially due to the viscosity difference (see Table I).

The pH = 14 tartronate (hydroxymalonate) dianion solution was investigated in the hope of generating another radical system which would be characterized by a single EPR transition (see Sec. IV E, below). Laroff and Fessenden[45] performed a pH study of this system and reported that the pK_a of the hydroxy proton in $HO\dot{C}(COO^-)_2$ is approximately 12.7. We consequently expected to find only the deprotonated form of this radical at pH 14. Unfortunately we discovered upon irradiation that three equally spaced lines (spacing about 7.3 G) were prominent in the spectrum, with an initial intensity ratio of approximately 1 : 2 : 1. Chemical decay of the high and low field lines was relatively slow (similar to the decay of the doubly charged malonate radical dianion), and a small amount of multiplet RPM polarization could be discerned. Chemical decay of the center line was much slower than even the outer lines, and we concluded that this transition belongs to the triply charged radical $^-O\dot{C}(COO^-)_2$ which was reported by Laroff and Fessenden.[45] We have assigned the remaining pair of lines to $^-O\dot{C}HCOO^-$, which must be formed by decarboxylation of tartronate with about the same yield as the hydrogen abstraction product. This radical has been observed and characterized previously in a radiolysis study of glycolic acid solutions.[46]

Dynamic saturation recovery experiments were performed on all three transitions in the tartronate system, with t_0 at 15, 45, and 75 μs following a 500 ns electron pulse, as part of the process of identifying the species present. It was found that the recovery times of the outer lines were on the order of 1.4 μs in all determinations. Because the g factor difference of the two radicals present is very small and the reaction rates are low, there should be no net RPM polarization of any transition. Consequently, we have used the sum of the outer line signals as a chemistry reference curve to determine T_1 for $^-O\dot{C}HCOO^-$. The procedure should be valid in this case even though two different radical species are present. The apparent recovery time of the center line increased from 2.8 to 3.4 to 3.5 μs as the time t_0 following radical creation was incremented. This behavior is clear evidence that the recovery curves are influenced by Heisenberg exchange, and we are presently only able to report that T_1 for $^-O\dot{C}(COO^-)_2$ is greater than 3.5 μs, although probably not more than 10% greater. Since the tartronate radical has only a single nuclear spin state, Heisenberg exchange in collisions between radicals of this species should not be observed.[10] The exchange behavior must be attributed to collisions between $^-O\dot{C}(COO^-)_2$ and $^-O\dot{C}HCOO^-$, which is the only case of Heisenberg exchange between dissimilar radicals which we have so far observed.

C. Alcohols

The α-hydroxyalkyl radicals formed from simple alcohols present some unique problems from the standpoint of FID-detected kinetics, because of the properties of the hydroxy proton. The pK_a of the α-hydroxy proton in these radicals falls in the range 9–12,[47] so that if one wants to study a single species contaminated by less than 1% of the other form, one must avoid the condition $pH = pK_a \pm 2$. The base-catalyzed proton exchange causes a significant line broadening,[45] and consequently the pH must be kept constant to avoid changes in the FID decay time. Finally, the

additional splitting [48] caused by the hydroxy proton significantly increases the width of the lines in $CH_3\dot{C}HOH$ and $(CH_3)_2\dot{C}OH$, and in $\cdot CH_2OH$ effectively creates pairs of closely spaced lines whose FID signals interfere.

Experimental conditions were chosen to overcome these problems. At pH = 14, only the deprotonated forms of the radicals are present, and the (deuterated) radicals formed in D_2O solution possess much smaller splitting constants. In concentrated phosphate buffer, the proton exchange rate is increased to approach an extreme narrowing limit where the hydroxy proton is effectively decoupled from the electron spin.[45] The buffer solution also served to maintain a constant pH near 7.0, since the radiolysis otherwise tends to increase the H_3O^+ concentration over the course of an experiment. The initial chemistry is not significantly altered in the buffer, since rates of hydrogen abstraction from alcohol are much greater than reaction of $\cdot OH$ with phosphate.[40]

The hydrogen abstraction reaction (R3) is known[43] to produce in excess of 85% α-hydroxyalkyl radical from ethanol and isopropanol, but with a significant fraction of β-hydroxy product. We failed to observe the β-hydroxy species, although we should have sufficient sensitivity to do so in the isopropanol system. Eiben and Fessenden[46] also noted their inability to detect the β-hydroxyisopropyl radical in their cw experiments. It is possible that T_2 for these radicals is less than 100 ns, in which case our FID integration method would not detect any signal.

The results compiled in Table I show that deuteration at the hydroxy position seems to produce very little effect on T_1. Hydroxyisopropyl radical was studied in phosphate buffer solution in both H_2O and D_2O, and the difference in T_1 is within the 10% experimental uncertainty (see Table I). In all other cases, protonated and deuterated radicals were formed in dissimilar solutions, and the differences in viscosity (Table I) can easily account for the variation in T_1. On the other hand, the T_1 of each deprotonated radical is much shorter than its protonated or deuterated analog. The differences cannot be entirely ascribed to a viscosity effect, and are probably correlated with the change in g factor between the two forms (see Sec. V).

In only one case have we studied the same radical ($\cdot CH_2OD$) at two significantly different temperatures. The T_1 increases by some 30% in going from 19 to 9 °C, which closely parallels the ~30% viscosity increase of water over the same temperature interval and tends to support a spin-rotation mechanism for relaxation of this radical (Sec. V).

The radical $\cdot CH_2O^-$ formed under high pH conditions deserves special mention, since it is the only free radical we have detected whose T_1 was too short to measure. Saturation recovery experiments were attempted, but the recovery was substantially complete within about 200 ns after the saturation pulse. The same result was obtained in both H_2O and D_2O solutions. Data obtained in this regime of very short delay time between pulses is unreliable because the probe pulse is distorted by the presence of the perturbation pulse, and the effective tip angle changes as the delay is scanned. An upper limit for T_1 of ~150 ns could be estimated. The FID decay time observed on an oscilloscope in this experiment was 100 ± 20 ns, so that a lower limit of 80 ns can be placed on T_1 and T_2. We have listed $T_1 \sim 0.1$ μs in Table I under the assumption that $T_1 = T_2$. Laroff and Fessenden[49] have published a spectrum of this radical which shows a linewidth on the order of 0.5 G, in good agreement with our observations. It is interesting to note that because of the short relaxation time, no report of CIDEP effects in the spectrum of $\cdot CH_2O^-$ has ever been made. We observed radical pair CIDEP in this system only at very short times after a tightly focused electron pulse. We were barely able to force the low field line into emission under our most extreme conditions of electron pulse length (2 μs) and beam intensity.

Very few other linewidth or T_1 measurements on transient hydroxyalkyl radicals have been reported to date, even though EPR detection of these radicals is quite common. Laroff and Fessenden[45] reported linewidths as a function of pH for the α-hydroxyethyl and α-hydroxyisopropyl radicals in a study of the proton exchange dynamics. The linewidths reported in their work are in qualitative agreement with the FID decay times we have observed. Recently Frydkjaer and Muus[50] reported $T_1 = 1.5$ μs for the hydroxyisopropyl radical in isopropanol at − 23 °C. Since the viscosity of isopropanol at − 23 °C is ~11 cP,[51] their result is compatible with ours (2.7 μs at ~1.5 cP) only if a different T_1 mechanism dominates under their much higher viscosity conditions. Paul[52] has reported $T_1 = 0.94$ μs for this radical in aqueous solution (pH = 9.2, 16 °C) based on cw progressive saturation experiments. This number is difficult to reconcile with our results, and we believe it to be at least 50% too low.

D. $\cdot CH_3$

The methyl radical is formed cleanly in aqueous solution by addition of $\cdot OH$ or $\cdot O^-$ to dimethyl sulfoxide,[42] and the free radical spectrum is characterized by a typical E/A (low field emission, high field absorption) multiplet CIDEP pattern at short times after the radiolysis pulse. The overall behavior shown in Fig. 5 for the + 1/2 and − 1/2 lines of $\cdot CH_3$ is very similar to the behavior of the $\cdot CH_2COO^-$ + 1 and − 1 lines, except that the time scale is shorter because both the reaction and spin relaxation are faster for methyl. We also observe a small signal (5% of the methyl signal) from a second radical in this system, which is characterized by a triplet spectrum with a 20.1 G splitting and a g factor virtually the same as methyl. The spectrum would be consistent with $\cdot CH_2SOCH_3$, which could be a product of hydrogen abstraction from DMSO by either $\cdot O^-$ or $\cdot H$.

Methyl is an important free radical both from practical and theoretical standpoints, but has been the subject of very few relaxation studies.[53,54] Zlochower *et al.*[54] measured the linewidth and proton hyperfine splittings as a function of temperature in aqueous solution, and found a width of about 0.8 G at room temperature, which was dominated by unresolvable second-order splitting. We observed a FID decay time of roughly 200 ns, which translates into a Lorentzian linewidth of 0.3 G. We also found $T_1 = 200$ ns, which shows $T_1 = T_2$ as expected. To our knowledge, there have been no other T_1 measurements on this important radical in solution, because of the obvious difficulties involved. Indeed, this experiment constitutes the shortest direct T_1 determination ever reported for a reactive free radical.

E. $\cdot SO_3^-$

The $\cdot SO_3^-$ radical produced in basic solutions of Na_2SO_3 is an important test case because it is characterized by zero nuclear spin and therefore only one EPR line. Other easily generated small free radicals with zero nuclear spin apparently relax too quickly for us to measure with the currently available apparatus.[55] When only a single line is present, Eq. (11) implies that the dynamic polarization recovery technique should give the proper T_1 result regardless of radical concentration, since there is no CIDEP or Heisenberg exchange contribution to the polarization.

In Fig. 6, we have plotted the apparent T_1 of $\cdot SO_3^-$ vs. apparent $T_c(t_0)$, which is defined as the second-order chemical half-life at the beginning of the recovery period. Data from several different experiments have been included in the plot. At sufficiently low concentration [$T_c(t_0) \geqslant 10\ \mu s$] we consistently obtain $T_1 \simeq 2.0\ \mu s$, regardless of the electron pulse duration or focusing conditions. We believe 2.0 μs is the true unimolecular T_1 for $\cdot SO_3^-$ in this solution, and we have included it in Table I.

Under the higher concentration conditions, there is a very significant trend toward *longer* T_1. This result is complete anomalous, since any bimolecular relaxation effects (Heisenberg exchange or electron dipole–dipole) should result in a *shorter* apparent T_1 at higher free radical concentration.[56] To rationalize the observation in terms of the discussion of Sec. II C, one must postulate that the unperturbed signal $S_{REF}(t)$ is positively enhanced ($P_z > 1$) for about 10 μs following either a tightly focused short (200 ns) electron pulse or a long (2 μs) diffused pulse, but that little enhancement develops for a short, diffused pulse. This behavior could be induced either by the reaction of $\cdot SO_3^-$ with primary radicals during the irradiation, or by reaction with other secondary radicals which are present but not observed. In either case the reaction must be with a radical which has a higher g factor than $\cdot SO_3^-$ ($g = 2.003\ 07$)[57] in order to give a positive enhancement.[10]

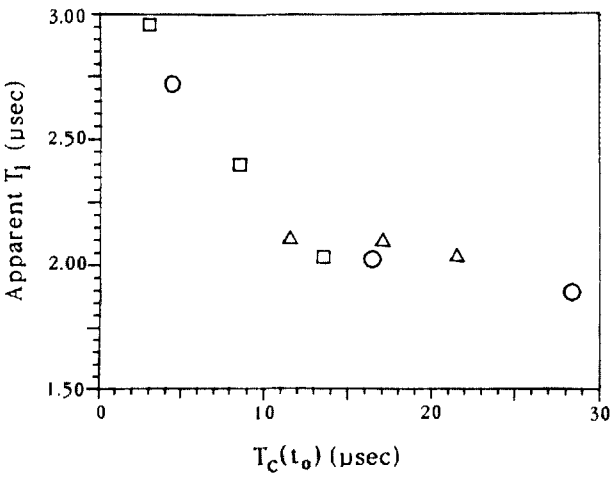

FIG. 6. Apparent T_1 measured as a function of chemical half-life [$T_c(t_0)$] for $\cdot SO_3^-$. Half-lives were estimated from the decay of each reference curve [$S_{REF}(t)$], by assuming that $S_{REF}(t) \propto R(t)$. Results from three different experiments are plotted: (a) tightly focused 200 ns electron pulse, saturation recovery method (circles); (b) diffused 100 ns electron pulse, inversion recovery method (triangles); (c) diffused 2.0 μs electron pulse, inversion recovery (squares).

Of the primary radical products of water radiolysis, H· may be immediately dismissed as a reaction partner because its g factor is lower than that of $\cdot SO_3^-$. Aqueous electron has a low g factor as well, but its reactions sometimes produce anomalous polarizations, possibly due to reaction into a triplet product state.[58] This was shown specifically *not* to be the case with $\cdot SO_3^-$, however.[58] Hydroxyl radical (or $\cdot O^-$) has a large g factor[48] but an extremely short T_1,[6] and enhancements from $\cdot OH$ or $\cdot O^-$ have never been reported. Moreover, the pseudo-first-order reaction rate of $\cdot O^-$ in 0.5 M $\cdot SO_3^=$ is $\sim 10^8\ s^{-1}$, which makes it inconceivable that significant reaction with $\cdot SO_3^-$ could take place.[41]

The radiation chemistry of $SO_3^=$ in 1.0 M NaOH solution has been studied previously,[41] and it is known that several other radicals are produced in the chain reactions of $\cdot SO_3^-$ with N_2O, HO_2^-, and O_2. The redox mechanism postulated by other workers[41,59] is given below in abbreviated form:

$$\cdot SO_3^- + N_2O \xrightarrow{2OH^-} SO_4^= + N_2 + \cdot O^-, \quad \text{(R7)}$$

$$\cdot SO_3^- \ HO_2^- \xrightarrow{OH^-} SO_3^= + \cdot O_2^-, \quad \text{(R8)}$$

$$\cdot SO_3^- + \cdot O_2^- \rightarrow SO_3^= + O_2, \quad \text{(R9)}$$

$$\cdot SO_3^- + O_2 \rightarrow \cdot SO_5^-, \quad \text{(R10)}$$

$$\cdot SO_5^- + SO_3^= \xrightarrow{2OH^-} 2SO_4^= + \cdot O^-. \quad \text{(R11)}$$

The Caro acid radical $\cdot SO_5^-$ should have a fairly high g factor (but a short relaxation time), and might be formed quickly in significant yield if the solution is contaminated with O_2. This seems unlikely, however, since the solution is naturally buffered against O_2 contamination by the chain oxidation itself. HO_2^- is formed in significant yield in water radiolysis of basic solutions,[37] but the rate of reaction (R8) is not known. If this reaction is close to diffusion controlled, then $\cdot O_2^-$ might be able to polarize the $\cdot SO_3^-$ radical transition. We are pursuing further experiments to determine the source of the $\cdot SO_3^-$ polarization.

We should point out that in principle the chain reactions involving N_2O and O_2 will contribute to the apparent T_1 and T_2 of $\cdot SO_3^-$ in this system, since the chain intermediate is $\cdot O^-$, which has a very short relaxation time. Every time an $\cdot SO_3^-$ radical reacts with N_2O or O_2, $\cdot O^-$ is formed and relaxes very quickly. Reaction of $\cdot O^-$ with $SO_3^=$ then forms a new $\cdot SO_3^-$ radical with a Boltzmann polarization probability. We have not observed any significant contribution from the O_2 chain reaction, presumably because the oxygen transfer reaction (R11) is relatively slow. Reaction (R7) was reported[41] to have a rate $k_8 = 3.5 \times 10^7\ M^{-1}\ s^{-1}$, which should give rise to $T_1 = T_2 \simeq 1.6 \times 10^{-6}$ s in a saturated N_2O solution. We have performed T_1 measurements in Ar-saturated solutions, however, and find $T_1 = 2.0\ \mu s$ as in the N_2O solution. We conclude, based on the maximum possible error in the measurements, that the reported rate constant is incorrect and an upper limit for k_8 is $\sim 10^6\ M^{-1}\ s^{-1}$, assuming $[N_2O]_{sat} = 0.02$ M.

V. MAGNITUDES OF RELAXATION TIMES

The primary purpose of this report is to describe procedures developed to accurately determine values of T_1 for highly reactive radicals. The data in Table I are consequently presented primarily as illustrations of the scope of the technique rather than as fundamental quantities to be discussed in their own right. Any detailed discussion of relaxation in these radicals will have to await the results of more extensive measurements, presently planned or in progress, in which temperature, viscosity, and, in some cases, isotopic content are varied. Nevertheless, the data in the table were obtained under sufficiently similar sets of conditions, and for a sufficiently homologous set of radicals, that some speculation about the principal relaxation mechanism operating for these species is irresistible.

We call attention to the following features of the relaxation times collected in Table I: (1) The values, ranging from 0.1 to 4 μs, are substantially shorter than the few T_1's known for larger reactive radicals. For example, benzyl[60] and hydroxydiphenylmethyl[22] radicals are reported to have T_1's of 8 and 20 μs, respectively, in media of viscosity comparable to that employed here. (2) The series of deprotonated ketyl radicals, $(CH_3)_nH_{2-n}CO^-$, have consistently shorter T_1's than the corresponding protonated forms, despite the fact that protonation should produce only a minor change in size. (3) The value for $\cdot CH_2OD$ *increases* by $\sim 30\%$ as the temperature *decreases* from 19 to 9 °C. The viscosity of H_2O increases by almost the same percentage over that temperature range. (4) The T_1's for $\cdot CH(CO_2^-)_2$ and $\cdot CH_2CO_2^-$ are the same for all hyperfine lines.

In the discussion below, it will be shown that these observations are consistent only with the spin-rotation mechanism for electron spin relaxation in these small radicals.

A. Criteria for short T_1

A convenient qualitative description of spin-lattice relaxation[1,61] within isolated radicals in fluid solution involves the assumption that random fields give rise to a mean-square distribution of Larmor frequencies, $\langle\omega^2\rangle$, experienced by the electron in the radical as it tumbles about in a manner describable by a spectral density function $J(\omega_0)$ where ω_0 is the resonance frequency ($\sim 6\times 10^{10}$ rad s^{-1} for X-band EPR). It is frequently found that $J(\omega_0)$ may be expressed in terms of a characteristic correlation time τ_c, and T_1 is given by[61,62]

$$T_1^{-1} = 2\langle\omega^2\rangle J(\omega_0) = \frac{2\langle\omega^2\rangle\tau_c}{1+\omega_0^2\tau_c^2}. \tag{36}$$

Numerous complications arise, of course, when there is some degree of correlation between the fluctuating fields and anisotropic molecular motion,[63] or when more than one type of spin is involved.[64] Even acknowledging the limitations of Eq. (36) for the radicals of interest here, however, it is still instructive to use it as a basis for considering the qualitative implications of an electron relaxation time of 10^{-6} s or less for such species.

One striking feature of Eq. (36) is the prediction that $1/T_1$ reaches its maximum value when $\omega_0\tau_c = 1$, thereby limiting T_1 to values longer than $\omega_0/\langle\omega^2\rangle^{1/2}$, or

$$T_1(\mu s) \geqslant 1.6\times 10^3[\langle\nu^2(\mathrm{MHz})\rangle]^{-1} \tag{37}$$

for X-band EPR. For variations in the Larmor frequency arising from rotational reorientation, the correlation time τ_c is usually approximated by[65]

$$\tau_c = v\eta/kT, \tag{38}$$

where v is a volume appropriate to the hydrodynamic radius of the molecule and η is the viscosity of the medium. For molecules with a specific gravity close to unity in H_2O at room temperature ($\eta = 1$ cP), we have

$$\tau_c(\mathrm{ps}) \cong 0.4\times \text{mol. wt.} \tag{39}$$

Consequently, the condition $\omega_0\tau_c = 1$ should be met for a radical with molecular weight of approximately 40, or roughly in the middle of the molecular weights represented by the radicals in Table I. Equations (36) and (38) therefore imply that the T_1's of these radicals should lie near their minimum possible values at the X-band EPR frequency. Larmor frequency variations on the order of 50–100 MHz are required, however, to account for T_1's in the observed range from 0.1 to 4 μs. Frequency fluctuations of this magnitude may arise due to g factor or hyperfine anisotropy, or the spin-rotation interaction. Sufficient data is available for several of the free radicals listed in Table I to warrant a more careful comparison of theory and experiment than is represented by Eqs. (36) and (38). Given below are more detailed predictions for $\cdot SO_3^-$, $\cdot CH(CO_2^-)_2$, and $\cdot CH_3$, which illustrate the predicted effects of the g factor anisotropy, hyperfine anisotropy, and spin-rotation mechanisms, respectively.

B. g-factor anisotropy: $\cdot SO_3^-$

Since the sulfite radical has no magnetic nuclei, hyperfine anisotropy cannot be a mechanism for relaxation. Other than spin rotation, the only strong remaining mechanism for relaxation in this radical should be due to anisotropy of the g tensor. For an isotropically tumbling radical, the relaxation time corresponding to this mechanism may be written as[66]

$$T_1^{-1} = (1/10)J(\omega_0)\omega_0^2(g':g'), \tag{40}$$

where $(g':g')$ is the inner product of the components of the anisotropic g tensor. In the principal axis system

$$(g':g') = (\Delta g_{xx})^2 + (\Delta g_{yy})^2 + (\Delta g_{zz})^2,$$

where $\Delta g_{xx} = g_{xx} - g_{\mathrm{iso}}$, etc. For $\cdot SO_3^-$ formed in an x-irradiated K_2SO_4 single crystal,[67] it was found that $\Delta g_{xx} = \Delta g_{yy} = 3.5\times 10^{-4}$ and $\Delta g_{zz} = 7\times 10^{-4}$. Substitution into Eq. (40) gives

$$T_1^{-1} = 2.9\times 10^{14} J(\omega_0). \tag{41}$$

The observed value of T_1 (2.0 μs) therefore requires that $J(\omega_0) = 1.7\times 10^{-9}$ s. *There is no real value of τ_c which could give this value of $J(\omega_0)$* if we assume the simple functional form $J(\omega_0) = \tau_c(1+\omega_0^2\tau_c^2)^{-1}$. This simply means that g factor anisotropy is too weak to account for a T_1 as short as that observed for $\cdot SO_3^-$. This is not surprising, since the effective value for $\langle\nu^2\rangle^{1/2}$ implied that Eq. (40) is ~ 2 MHz, i.e., more than an order of magnitude lower than required for a T_1 of 10^{-6} s. It is clear that a stronger mechanism (presumably spin rotation) must be responsible for the T_1 of $\cdot SO_3^-$.

C. Hyperfine anisotropy: $\cdot CH(CO_2^-)_2$

Addition of even one magnetic nucleus to a radical leads to a considerably more complex description of spin-lattice relaxation than that given above. One must consider transitions not just of the electron spin, but must allow for nuclear spin transitions as well.[61–68] We consider here only the simplest case, that of a radical with a single proton. Table I contains two examples of this spin system: $\cdot CH(CO_2^-)_2$ and $^-OCHCO_2^-$. Because of its higher symmetry, which assures the same principal axis system for the g and hyperfine tensors, we will consider only the malonate radical, $\cdot CH(CO_2^-)_2$.

Let us label the four combined electron–nuclear spin states as follows, in the approximate order of increasing energy:

$$|1\rangle = |\beta_e\alpha_H\rangle,$$
$$|2\rangle = |\beta_e\beta_H\rangle,$$
$$|3\rangle = |\alpha_e\alpha_H\rangle,$$
$$|4\rangle = |\alpha_e\beta_H\rangle.$$

The transition probabilities W_{kl} among these four states under the combined action of g factor and hyperfine anisotropy in an isotropically tumbling radical will be given by[23,66]

$$\begin{aligned}
W_{13} &= W_e^+ = (1/20)[\omega_e^2(g':g') \\
&\quad + \omega_e(g':A') + (1/4)(A':A')]J(\omega_e), \\
W_{24} &= W_e^- = (1/20)[\omega_e^2(g':g') \\
&\quad - \omega_e(g':A') + (1/4)(A':A')]J(\omega_e), \\
W_{12} &= W_{34} = W_H = (1/80)[(A':A')]J(\omega_H), \\
W_{14} &= W_0 = (1/120)[(A':A')]J(\omega_e - \omega_H), \\
W_{23} &= W_2 = (1/20)[(A':A')]J(\omega_e + \omega_H). \qquad (42)
\end{aligned}$$

By analogy with Eq. (40), $(A':A')$ is the inner product of the anisotropic hyperfine tensor (in rad s^{-1}) and $(g':A')$ is the cross product between g factor and hyperfine anisotropies. The electron and proton Larmor frequencies are designated in this case as ω_e and ω_H, respectively. Since $\omega_e \gg \omega_H$, we may equate $J(\omega_e)$ and $J(\omega_e \pm \omega_H)$ and let $J(\omega_H) = J(0)$. We are also concerned here with estimating the maximum values of the transition probabilities. As described above, the spectral density function will generally have its maximum when $\omega_e\tau_c = 1$. Under this condition, $J(0) = 2J(\omega_e) = \omega_e^{-1}$. The inner products may be determined from the known g factor and hyperfine anisotropies for malonate radical.[69,70] Thus

$$(g':g') = 2.1\times10^{-6};\ (g':A')\omega_e^{-1} = -2.8\times10^{-6};$$
$$(A':A')\omega_e^{-2} = 17.5\times10^{-6}.$$

The transition probabilities from Eq. (42) may be incorporated into the equations of motion which describe the decay of the intensities of the two EPR transitions, S^+ and S^-, and the two NMR transitions, I^+ and I^-, toward their equilibrium values, S^0 and I^0. For the case of one electron and one proton, the problem reduces to solving three simultaneous equations[71]:

$$(d/dt)\begin{bmatrix} S \\ \Delta \\ I \end{bmatrix} = -\begin{bmatrix} \rho_e & \delta & \sigma \\ \delta & \mu & 0 \\ \sigma & 0 & \rho_H \end{bmatrix}\begin{bmatrix} S \\ \Delta \\ I \end{bmatrix}, \qquad (43)$$

where

$$\begin{aligned}
S &= [|1\rangle \rightarrow |3\rangle] + [|2\rangle \rightarrow |4\rangle] \\
&= (S^+ - S^0) + (S^- - S^0), \\
\Delta &= [|1\rangle \rightarrow |3\rangle] - [|2\rangle \rightarrow |4\rangle] = (S^+ - S^-), \\
I &= [|1\rangle \rightarrow |2\rangle] + [|3\rangle \rightarrow |4\rangle] = (I^+ - I^0) + (I^- - I^0),
\end{aligned}$$

and

$$\begin{aligned}
\rho_e &= W_2 + W_e^+ + W_e^- + W_0 \quad = 5.0\times10^4\ s^{-1}, \\
\rho_H &= W_2 + 2W_H + W_0 \quad = 5.7\times10^4\ s^{-1}, \\
\delta &= W_e^+ - W_e^- \quad = -0.85\times10^4\ s^{-1}, \\
\sigma &= W_2 - W_0 \quad = 2.2\times10^4\ s^{-1}, \\
\mu &= W_e^+ + W_e^- + 2W_H \quad = 4.6\times10^4\ s^{-1}.
\end{aligned}$$

The estimated values of ρ_e, etc. are given for the limit where $\omega_e\tau_c = 1$.

Equations (43) have been solved to yield the saturation recovery curves $S^+(t)$ and $S^-(t)$ for the high and low field EPR lines of malonate, respectively, assuming $S^+(0) = S^0$ when $S^-(0) = 0$ and vice versa, and that $I(0) = 0$. The recovery time t is given in μs.

$$\begin{aligned}
S^+(t) &= S^0\{1 - [0.61\exp(-0.076t) + 0.28\exp(-0.047t) \\
&\quad + 0.11\exp(-0.029t)]\}, \\
S^-(t) &= S^0\{1 - [0.58\exp(-0.047t) + 0.35\exp(-0.076t) \\
&\quad + 0.07\exp(-0.029t)]\}. \qquad (44)
\end{aligned}$$

Three aspects of the relaxation behavior predicted for malonate radical by Eq. (44) are obvious: (1) The relaxation of neither line can be described theoretically in terms of a single relaxation time, (2) the time dependence of the recovery curves should be different for the two transitions, and (3) the fastest of the three recovery times, $(0.076)^{-1} = 13\ \mu$s, is still $\sim$5 times slower than the observed T_1 (2.9 μs). While the nonexponential nature of the recovery predicted by Eq. (44) is nearly undetectable in plots of $[S^\pm(t) - S^0]$ vs time, the predicted pseudoexponential relaxation times evaluated from plots of S^+ and S^- give values of $\sim$20 and 27 μs, respectively. Thus, the combined g factor and hyperfine anisotropy mechanisms predict a 30% difference between the recovery times for the high and low field lines. This difference is well outside the estimated error of 10% for the relaxation time measurements. It should also be pointed out that the expected difference in relaxation behavior for the two lines is relatively insensitive to either the functional form or value of $J(\omega_e)$, since it results from the fact that W_e^+ and W_e^- have different values. It thus seems clear that neither the short observed T_1 for malonate nor the identical T_1 for both of its hyperfine lines can be accounted for by g factor or hyperfine anisotropy mechanisms.

It is similarly found that the T_1's for the three hyperfine lines of $\cdot CH_2CO_2^-$ are the same to within 10%. This is qualitatively inconsistent with a dominant dipolar mechanism

since this would lead to the expectation of slower relaxation for the center line than for the outer lines.[64,72] Since the other protonated radicals in Table I should have hyperfine anisotropies comparable to those for malonate and acetate, it appears that this mechanism is too weak to explain *any* of the T_1's reported here.

D. Spin-rotation interaction: $\cdot CH_3$

The g factor anisotropy of methyl radical is substantially smaller than that for $\cdot SO_3^-$, and its proton hyperfine anisotropy exceeds that of malonate by less than a factor of 2.[73,74] Yet the observed value of T_1 for methyl is tenfold *shorter* than for either of these radicals. Given the failure of the g factor and hyperfine mechanisms to account for relaxation in the first two cases, it is pointless to apply either of these mechanisms to methyl. We turn instead to the only remaining common mechanism proposed for electron relaxation in radicals in solution: the spin-rotation mechanism which operates via the spin-rotation interaction, $H_{SR} = J \cdot C \cdot S$, where J is the total angular momentum of the radical.[75] Methyl radical is particularly suitable for such an estimate because its spin-rotation coupling tensor C has been measured recently using high resolution vibrational spectroscopy in the gas phase.[76,77]

The spin-rotation contribution to T_1 for an axially symmetric radical may be estimated from the formula[78]

$$T_1^{-1} = (2kT/3\hbar^2)[C_\parallel^2 I_\parallel + 2C_\perp^2 I_\perp]\tau_J, \tag{45}$$

where $C_\parallel$ and $C_\perp$ are the components of the spin-rotation coupling tensor parallel and perpendicular to the threefold axis of symmetry, $I_\parallel$ and $I_\perp$ are the corresponding moments on inertia, and τ_J is the angular momentum correlation time. Equation (45) has been derived on the assumption that (1) the molecule undergoes isotropic angular momentum diffusion, and (2) that τ_J^{-1} is greater than τ_c^{-1}, ω_0, and the average frequency of rotation about any of the axes K, $(kT/I_K)^{1/2}$. To test these conditions, we may use the known values of C_K, I_K, and T_1 in Eq. (45) to estimate the value of τ_J. From the work of Yamada *et al.*[76] we know that $C_\perp = 330$ MHz, and $C_\parallel < 30$ MHz. Given that $I_\parallel = 2I_\perp = 1.93\times10^{-40}$ g cm^2 and $T_1 = 0.2\times10^{-6}$ s (Table I) we estimate

$$\tau_J^{-1} = 1.0\times10^{11}\ \text{s}^{-1}$$

for $\cdot CH_3$ in 1 M NaOH at 19 °C. This barely satisfies the condition relative to ω_0 ($= 6\times10^{10}$ rad s^{-1}), marginally fails the condition for τ_c^{-1} [$= 1.7\times10^{11}$ s^{-1}, estimated from Eq. (39)], and flunks the test for average frequency of rotation about any of the axes K, $(kT/I_\parallel)^{1/2}$ ($= 1.4\times10^{13}$ s^{-1}). Although Eq. (45) has been modified to allow for the breakdown in the last condition,[79] we defer more refined estimates of T_1 for methyl. Such refinements must not only allow for the low moment of inertia for $\cdot CH_3$, but need also to explore the effects of anisotropy in both reorientation and angular momentum diffusion[80–83] and the possibility that reorientation of a small molecule like methyl in a structured solvent like H_2O actually occurs faster than the change in the magnitude of J (M diffusion vs. J diffusion).[84]

Even in the absence of such refinements, it seems clear that the spin-rotation mechanism comes closer than any other to explaining the short relaxation time for $\cdot CH_3$ in H_2O. It is reasonable to assume that this mechanism also accounts for the short T_1's for the other radicals in Table I. Although the spin-rotation constants for these radicals have not been, and in most cases probably will not be, determined directly, estimates of C based on g factors and moments of inertia can be made and applied to the T_1's via Eq. (45) or its modifications.[85] Thus, the consistently shorter T_1's for the ketyl anions $(CH_3)_nH_{2-n}CO^-$, relative to their protonated analogs, are consistent with the greater observed g factors, and larger expected spin-rotation constants, for the former species. In a similar vein, the increase of T_1^{-1} with decreasing (η/T) for $\cdot CH_2OD$ is consistent with the Hubbard model which predicts an increase in τ_J with this parameter.[86,87] More detailed estimates of T_1 due to the spin-rotation mechanism will be better compared, however, with T_1's obtained over a range of (η/T). Such studies are in progress.

VI. CONCLUSION

In summary, we have demonstrated a dynamic polarization recovery method for T_1 measurement in short-lived free radicals which are generated in short pulses. By performing two or three EPR kinetics experiments on the same chemical system, T_1 information may be reliably extracted following simple manipulation of the data. Signal-to-noise ratio is improved over other techniques since one can take full advantage of the large radical populations and CIDEP signal enhancements typically created in a pulsed radiolysis experiment. The greatest advantage of the method lies in the fact that knowledge of the microwave field amplitude at the sample is unnecessary. Measurement of this quantity in more conventional experiments is notoriously difficult.

Dynamic polarization recovery using the FID detection technique is especially appropriate for small reactive free radicals with short relaxation times and simple EPR spectra such as those listed in Table I. Our analysis has shown that the measured T_1's are near the minimum possible relaxation times for X-band EPR, and that spin rotation is the dominant spin-lattice relaxation mechanism. The dynamic properties in solution of these species are of great theoretical interest, since the radicals may ultimately be used as probe of the liquid structure. More systematic studies of temperature, viscosity, and microwave frequency effects are needed, however, in order to adequately test the available theory.

Although we have developed dynamic polarization recovery for T_1 measurements in free radical systems created by pulse radiolysis, there is no reason the method cannot be used in photolysis experiments as well. The primary requirement, when second-order kinetics plays a dominant role, is that the light pulses be reproducible from shot to shot. Relatively inexpensive excimer lasers with high pulse energies and excellent stability are now becoming available. Such equipment should greatly extend the range of chemical systems which can be studied using the technique. In particular, we look forward to solvent and temperature studies on small reactive free radicals such as $\cdot CH_3$ and $\cdot SO_3^-$, which should enhance the basic understanding of rotational reorientation processes in liquids.

ACKNOWLEDGMENTS

The authors wish to acknowledge Pat Walsh and Bob Clarke, who performed viscosity measurements. We also wish to thank the Van de Graaff operators R. E. Lowers and A. Youngs for their assistance.

[1]See *Electron Spin Relaxation in Liquids*, edited by L. T. Muus and P. W. Atkins (Plenum, New York, 1972) for articles on several of these topics.
[2]G. I. Likhtenstein, *Spin Labeling Methods in Molecular Biology* (Wiley, New York, 1976).
[3]J. S. Hyde, in *Time Domain Electron Spin Resonance*, edited by L. Kevan and R. N. Schwartz (Wiley, New York, 1979).
[4]S. K. Rengan, M. P. Khakhar, B. S. Prabhananda, and B. Venkataraman, Pure Appl. Chem. **32**, 287 (1972).
[5]J. B. Pedersen, J. Chem. Phys. **59**, 2656 (1973).
[6]N. C. Verma and R. W. Fessenden, J. Chem. Phys. **65**, 2139 (1976).
[7]A. D. Trifunac, J. R. Norris, and R. G. Lawler, J. Chem. Phys. **71**, 4380 (1979).
[8]A. D. Trifunac and R. G. Lawler, Chem. Phys. Lett. **84**, 515 (1981).
[9]C. D. Buckley, A. I. Grant, K. A. McLauchlan, and A. J. D. Ritchie, Faraday Discuss. Chem. Soc. **78**, 1 (1984).
[10]J. H. Freed and J. B. Pedersen, Adv. Magn. Reson. **8**, 1 (1976).
[11]J. A. Syage, R. G. Lawler, and A. D. Trifunac, J. Chem. Phys. **77**, 4774 (1982).
[12]J. A. Syage, Ph.D. thesis, Brown University, Providence, RI, 1982.
[13]R. W. Fessenden, J. Chem. Phys. **58**, 2489 (1973).
[14]C. P. Poole, Jr., *Electron Spin Resonance* (Wiley, New York, 1983).
[15]A. D. Trifunac and M. C. Thurnauer, in *Time Domain Electron Spin Resonance*, edited by L. Kevan and R. N. Schwartz (Wiley, New York, 1979).
[16]P. W. Atkins, K. A. McLauchlan, and A. F. Simpson, J. Phys. E **3**, 547 (1970).
[17]N. C. Verma, Ph.D. thesis, Carnegie-Mellon University, Pittsburgh, PA, 1975.
[18]J. W. M. DeBoer, T. Y. C. Chan Chung, and J. K. S. Wan, Can. J. Chem. **57**, 2971 (1979).
[19]R. W. Fessenden, J. P. Hornak, and B. Venkataraman, J. Chem. Phys. **74**, 3694 (1980).
[20]P. W. Atkins, K. A. McLauchlan, and P. W. Percival, Mol. Phys. **25**, 281 (1973).
[21]K. A. McLauchlan, R. C. Sealy, and J. M. Wittmann, Mol. Phys. **35**, 51 (1978).
[22]K. A. McLauchlan, R. C. Sealy, and J. M. Wittmann, Mol. Phys. **36**, 1397 (1978).
[23]P. J. Hore, K. A. McLauchlan, L. Pasimeni, and R. C. Sealy, J. Chem. Soc. Faraday Trans. 2 **74**, 1662 (1978).
[24]P. J. Hore and K. A. McLauchlan, J. Magn. Reson. **36**, 129 (1979).
[25]P. J. Hore and K. A. McLauchlan, Mol. Phys. **42**, 533 (1981).
[26]P. J. Hore and K. A. McLauchlan, Mol. Phys. **42**, 1009 (1981).
[27]K. A. McLauchlan and G. R. Sealy, Mol. Phys. **52**, 783 (1984).
[28]H. Paul, Chem. Phys. **87**, 73 (1984).
[29]This assumption is certainly valid for non-spin-selective reactions, but may not be strictly correct for spin-dependent radical combination reactions. Further work on this point is in progress.
[30]C. P. Slichter, *Principles of Magnetic Resonance* (Springer, New York, 1978).
[31]D. M. Bartels, A. D. Trifunac, and R. G. Lawler (in preparation).
[32]Equation (7) may be obtained by straightforward substitution of Eqs. (2) and (3) into Eq. (1a) of Ref. 11.
[33]As shown in Sec. IV, this assumption is very good for small free radicals in solvents of low viscosity.
[34]H. C. Torrey, Phys. Rev. **76**, 1059 (1949).
[35]E. T. Jaynes, Phys. Rev. **98**, 1099 (1955).
[36]A. K. Saha and T. P. Das, *Theory and Applications of Nuclear Induction* (Saha Institute of Nuclear Physics, Calcutta, India, 1957).
[37]J. W. T. Spinks and R. J. Woods, *An Introduction to Radiation Chemistry* (Wiley, New York, 1964).
[38]M. Anbar, M. Bambenek, and A. B. Ross, Natl. Stand. Ref. Data Ser. Natl. Bur. Stand. 43 (1973).
[39]M. Anbar, Farhataziz, and A. B. Ross, Natl. Stand. Ref. Data Ser. Natl. Bur. Stand. 51 (1975).
[40]Farhataziz and A. B. Ross, Natl. Stand. Ref. Data Ser. Natl. Bur. Stand. 59 (1977).
[41]Z. P. Zagorski, K. Sehested, and S. O. Nielsen, J. Phys. Chem. **75**, 3510 (1971).
[42]D. Veltwisch, E. Janata, and K. D. Asmus, J. Chem. Soc. Perkin Trans. 2 **1980**, 146.
[43]A. J. Swallow, Prog. React. Kinet. **9**, 195 (1979).
[44]D. M. Bartels, R. G. Lawler, and A. D. Trifunac, J. Magn. Reson. **54**, 507 (1983).
[45]G. P. Laroff and R. W. Fessenden, J. Phys. Chem **77**, 1283 (1973).
[46]K. Eiben and R. W. Fessenden, J. Phys. Chem. **75**, 1186 (1971).
[47]K. D. Asmus, A. Henglein, A. Wigger, and G. Beck, Ber. Bunsenges. Phys. Chem. **70**, 756 (1966).
[48]*Magnetic Properties of Free Radicals*, Vol. 9 in New Series, Group II, Landolt-Börnstein, edited by H. Fischer and K.-H. Hellwege (Springer, Berlin, 1977).
[49]G. P. Laroff and R. W. Fessenden, J. Chem. Phys. **57**, 5614 (1972).
[50]S. Frydkjaer and L. T. Muus, Chem. Phys. **59**, 365 (1981).
[51]R. W. Gallant, *Physical Properties of Hydrocarbons* (Gulf, Houston, 1968), Vol. 1.
[52]H. Paul, Chem. Phys. **40**, 265 (1979).
[53]J. Michalik and L. Kevan, J. Chem Phys. **68**, 5325 (1978).
[54]I. A. Zlochower, W. R. Miller, and G. K. Fraenkel, J. Chem. Phys. **42**, 3339 (1965).
[55]D. Behar and R. W. Fessenden, J. Phys. Chem. **76**, 1706 (1972).
[56]G. J. Kruger, Adv. Mol. Relaxation Processes **3**, 235 (1972).
[57]O. P. Chawla, N. L. Arthur, and R. W. Fessenden, J. Phys. Chem. **77**, 772 (1973).
[58]R. W. Fessenden and N. C. Verma, J. Am. Chem. Soc. **98**, 243 (1976).
[59]E. Hayon, A. Treinin, and J. Wilf, J. Am. Chem. Soc. **94**, 47 (1972).
[60]R. Baer and H. Paul, Chem. Phys. **87**, 73 (1984).
[61]N. Bloembergen, E. M. Purcell, and R. V. Pound, Phys. Rev. **73**, 679 (1948).
[62]A. Abragam, *The Principles of Nuclear Magnetism* (Oxford University, London, 1961).
[63]This seems first to have been recognized for the case of nuclear magnetic relaxation: D. E. Woessner, J. Chem. Phys. **37**, 647 (1962); H. Shimizu, *ibid.* **37**, 765 (1962); **40**, 754 (1964).
[64]J. H. Freed and G. K. Fraenkel, J. Chem. Phys. **39**, 326 (1963).
[65]Relationships between correlation times and molecular properties have been most extensively developed for nuclear relaxation. See, for example, R. T. Obermyer and E. P. Jones, J. Chem. Phys. **58**, 1677 (1973); J. DeZwaan and J. Jonas, *ibid.* **63**, 4606 (1975); M. Fury and J. Jonas, *ibid.* **65**, 2206 (1976).
[66]A. Carrington and A. D. McLachlan, *Introduction to Magnetic Resonance* (Harper and Row, New York, 1967).
[67]V. V. Gromov and J. R. Morton, Can. J. Chem. **44**, 527 (1966).
[68]J. H. Freed, D. S. Leniart, and J. S. Hyde, J. Chem. Phys. **47**, 2762 (1967).
[69]H. M. McConnell, C. Heller, T. Cole, and R. W. Fessenden, J. Am. Chem. Soc. **82**, 776 (1960).
[70]A. Horsfield, J. R. Morton, and D. H. Whiffen, Mol. Phys. **4**, 327 (1961).
[71]These equations reduce to the more familiar ones for two spin 1/2 nuclei when $W_e^+ = W_e^-$: E. L. Mackor and C. MacLean, J. Chem. Phys. **42**, 4254 (1965); C. L. Mayne, D. W. Alderman, and D. M. Grant, *ibid.* **63**, 2514 (1975).
[72]This is related to the well-known M_I^2 dependence of the width of hyperfine lines in the presence of hyperfine anisotropy: H. M. McConnell, J. Chem. Phys. **25**, 709 (1956).
[73]M. T. Rogers and L. D. Kispert, J. Chem. Phys. **46**, 221 (1967).
[74]M. Barfield, A. S. Babaqi, D. M. Doddrell, and H. P. W. Gottlieb, Mol. Phys. **42**, 153 (1981).
[75]For a discussion of the early evidence for the spin-rotation mechanism of relaxation, see P. W. Atkins and D. Kivelson, J. Chem. Phys. **44**, 169 (1966).
[76]C. Yamada, E. Hirota, and K. Kawaguchi, J. Chem. Phys. **75**, 5256 (1981).
[77]V. Spirko and P. R. Bunker, J. Mol. Spectrosc. **95**, 381 (1982).
[78]P. W. Atkins, Mol. Phys. **12**, 133 (1967).

[79]R. E. D. McClung, J. Chem. Phys. **57**, 5478 (1972).
[80]J. H. Freed, J. Chem. Phys. **41**, 2077 (1964).
[81]P. S. Hubbard, Phys. Rev. A **6**, 2421 (1972).
[82]P. S. Hubbard, Phys. Rev. A **8**, 1429 (1973).
[83]P. S. Hubbard, Phys. Rev. A **9**, 481 (1974).
[84]R. G. Gordon, J. Chem. Phys. **44**, 1830 (1966).
[85]R. F. Curl, Mol. Phys. **9**, 585 (1965).
[86]P. S. Hubbard, Phys. Rev. **131**, 1155 (1963).
[87]For experimental verification of this effect for paramagnetic complexes, see R. Wilson and D. Kivelson, J. Chem. Phys. **44**, 154, 4445 (1966).